The Heteronuclear Cluster Chemistry of the Group 1B Metals. Part 1. Structural Similarities and Differences Among Mixed-metal Cluster Compounds containing Copper, Silver, or Gold Atoms ligated by Phosphines. *X*-Ray Crystal Structures of $[CuRu_4(\mu_3\text{-}H)_3(CO)_{12}(PMePh_2)]$ and $[CuRu_3(CO)_9(C_2Bu^t)(PPh_3)]$ *

Robert A. Brice, Sheena C. Pearse, and Ian D. Salter
Department of Chemistry, University of Exeter, Exeter EX4 4QD
Kim Henrick
School of Chemistry, The Polytechnic of North London, London N7 8DB

Treatment of dichloromethane solutions of $[N(PPh_3)_2][Ru_4(\mu\text{-}H)_3(CO)_{12}]$ or $[N(PPh_3)_2][Ru_3(CO)_9(C_2Bu^t)]$ with $[M(NCMe)_4]PF_6$ (M = Cu or Ag) at −30 °C, followed by the addition of the desired phosphine ligand, affords the mixed-metal clusters $[MRu_4(\mu_3\text{-}H)_3(CO)_{12}L]$ [M = Cu, L = $PMePh_2$ (**1**) or PPh_3 (**2**); M = Ag, L = PPh_3 (**3**)], $[\{MRu_4(\mu_3\text{-}H)_3(CO)_{12}\}_2(\mu\text{-}Ph_2PCH_2CH_2PPh_2)]$ [M = Cu (**6**) or Ag (**7**)], and $[MRu_3(CO)_9(C_2Bu^t)(PPh_3)]$ [M = Cu (**10**) or Ag (**11**)] in *ca.* 70—80% yield. In dichloromethane solution, $[N(PPh_3)_2][Ru_4(\mu\text{-}H)_3(CO)_{12}]$, $[N(PPh_3)_2][Ru_3(CO)_9(C_2Bu^t)]$, and $[N(PPh_3)_2][Fe_3(\mu\text{-}COMe)(CO)_{10}]$ also react directly with $[MX(PPh_3)]$ (M = Cu or Au, X = Cl; M = Ag, X = I) or $[Au_2(\mu\text{-}Ph_2PCH_2PPh_2)Cl_2]$, in the presence of $TlPF_6$, to give reduced yields of (**2**), (**3**), (**10**), and (**11**), two analogous gold–ruthenium clusters $[AuRu_4(\mu\text{-}H)_3(CO)_{12}(PPh_3)]$ (**8**) and $[\{AuRu_4(\mu\text{-}H)_3(CO)_{12}\}_2(\mu\text{-}Ph_2PCH_2PPh_2)]$ (**9**), and the series of clusters $[MFe_3(\mu\text{-}COMe)(CO)_{10}(PPh_3)]$ [M = Cu (**15**), Ag (**16**), or Au (**17**)], as appropriate. All of these clusters have been characterized by i.r. and n.m.r. spectroscopy and the structures of (**1**) and (**10**) have been established by single-crystal *X*-ray diffraction studies. Clusters (**8**) and (**9**) adopt different metal-core structures to those of (**1**)—(**3**), (**6**), and (**7**), with the $Au(PR_3)$ (R = alkyl or aryl) fragment(s) in (**8**) and (**9**) bridging an edge of a ruthenium tetrahedron, whereas the $M(PR_3)$ (M = Cu or Ag) unit(s) in (**1**)—(**3**), (**6**), and (**7**) cap a face of a similar basic Ru_4 tetrahedron. However, clusters (**15**), (**16**), and (**17**) all have the same skeletal geometry, with the $M(PPh_3)$ (M = Cu, Ag, or Au) groups bridging an edge of an iron triangle, and species (**10**) and (**11**) show the same 'butterfly' metal-core arrangement as that previously established for the analogous gold species $[AuRu_3(CO)_9(C_2Bu^t)(PPh_3)]$. The pentanuclear cluster $[CuRu_4(\mu_3\text{-}H)_3(CO)_{12}(PMePh_2)]$ (**1**) has a trigonal-bipyramidal metal-core geometry, with the copper atom occupying an apical site [Cu–Ru 2.717(1)—2.749(1), Ru–Ru 2.788(1)—2.970(1) Å]. Each ruthenium atom is ligated by three terminal CO groups and the copper atom by the $PMePh_2$ ligand. All three $CuRu_2$ faces of the metal skeleton are capped by triply-bridging hydrido ligands [mean Cu–H 1.93(6), mean Ru–H 1.81(6) Å]. The tetranuclear cluster $[CuRu_3(CO)_9(C_2Bu^t)(PPh_3)]$ (**10**) adopts a 'butterfly' metal-core structure (interplanar angle 115.7°), with the copper atom occupying a 'wing-tip' site. The two Cu–Ru bond lengths are equal [2.603(1) Å] and the side of the Ru_3 triangle which is bridged by the $Cu(PPh_3)$ fragment [2.762(1) Å] is significantly shorter than the other two Ru–Ru distances [2.819(1) and 2.808(1) Å]. The t-butylacetylide ligand lies on the convex side of the 'butterfly' metal core, interacting with all three ruthenium atoms *via* one σ bond to the 'wing-tip' ruthenium site and two π bonds to the two ruthenium atoms which form the 'body' of the 'butterfly'. Each ruthenium atom is ligated by three CO groups, two of which also exhibit short Cu–C contacts [2.496(7) and 2.552(7) Å].

In the last five years, heteronuclear cluster compounds containing one or more $Au(PR_3)$ (R = aryl or alkyl) units have attracted a great deal of attention.[1] For mixed-metal gold clusters containing only one $Au(PR_3)$ moiety, it has been found that this unit either adopts a bonding mode in which it bridges a metal–metal bond or it caps a triangular three-metal face. Moreover, in almost all of the compounds where structural comparisons are possible, the $Au(PR_3)$ fragment occupies a similar position to that of the isolobal hydrido ligand in the related hydridometal cluster.[1] The situation is much more complicated for heteronuclear clusters containing more than one $Au(PR_3)$ unit, however. Although the $Au(PR_3)$ groups still normally adopt edge- or face-bridging bonding modes, cases of these moieties assuming the positions of hydrido ligands are the exceptions rather than the normal rule. A wide variety of structural types are known,[1,2] ranging from examples of clusters containing one or more gold–gold bonds to clusters where there is definitely no interaction between the gold atoms. For some

* 2,2,2,3,3,3,4,4,4,5,5,5-Dodecacarbonyl-1,2,3;1,2,4;1,3,4-tri-μ_3-hydrido-1-(methyldiphenylphosphine)-*cyclo*-coppertetraruthenium(6 *Ru–Ru*)(3 *Cu–Ru*) and μ_3-[t-butylethynyl-C^1($Ru^{1,3}$),C^2($Ru^{1,2}$)]-1,1,1,2,2,2,3,3,3-nonacarbonyl-1,2-μ-[(triphenylphosphine)cuprio]-*triangulo*-triruthenium, respectively.

Supplementary data available (No. SUP 56598, 9 pp.): thermal parameters, H-atom positional parameters. See Instructions for Authors, *J. Chem. Soc., Dalton Trans.*, 1986, Issue 1, pp. xvii–xx. Structure factors are available from the editorial office.

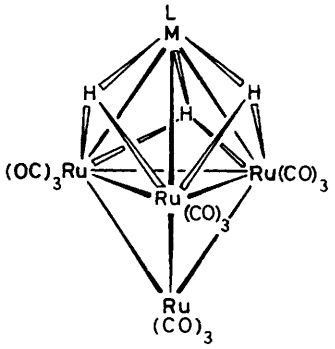

M L
(1) Cu $PMePh_2$
(2) Cu PPh_3
(3) Ag PPh_3
(4) Cu NCMe
(5) Ag NCMe

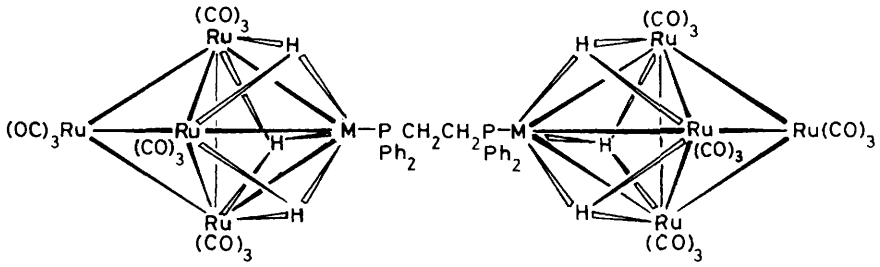

M
(6) Cu
(7) Ag

structures, the internuclear separations are such that whether a direct gold–gold linkage is present or not is arguable.[1,2] However, despite the great recent interest shown in these gold heteronuclear clusters, relatively few examples of analogous copper or silver compounds have been reported and, in comparison to the $Au(PR_3)$ group, very little experimental evidence concerning the cluster bonding capabilities of $M(PR_3)$ (M = Cu or Ag) fragments is available.

Our interest in trying to obtain such information was stimulated by theoretical studies on the cluster bonding capabilities of the $M(PR_3)$ (M = Cu, Ag, or Au) moieties. Evans and Mingos[3] have shown that the frontier molecular orbitals, which have a predominance of *d* orbital character, are filled and that the bonding characteristics of these units are determined primarily by the hybrid(*s*-*z*) orbital (a_1 symmetry) and a higher lying degenerate pair of p_x and p_y orbitals (*e* symmetry). However, although the calculations suggest that the $Cu(PR_3)$ fragment can be considered to be isolobal with a $Mn(CO)_3$ group, because their frontier molecular orbital energies are approximately the same, in the case of the $Au(PR_3)$ moiety, the p_x and p_y orbitals are much higher in energy and play only a secondary bonding role. Thus, the $Au(PR_3)$ unit approximates to being isolobal with a $Mn(CO)_5$ fragment or a hydrido ligand. According to the calculations of Mingos,[4] the $Au(PR_3)$ fragment effectively functions as $Au(PR_3)^+$ in heteronuclear clusters and both the face-capping and the edge-bridging bonding modes adopted by this moiety result in an increment of 12 to the polyhedral electron count. The high lying a_1 and *e* frontier orbitals of a capping $Au(PR_3)$ group are destabilized by the interactions with a triangular metal face so that they are not available for skeletal bonding. When the $Au(PR_3)$ unit bridges a metal–metal bond, it utilizes its a_1 hybrid(*s*-*z*) orbital in a three-centre, two-electron bonding interaction and the *e* set of p_x and p_y orbitals are too high lying in energy to make an effective contribution. However, the $Cu(PR_3)$ fragment is isolobal with the $Mn(CO)_3$ unit[3] and the latter does not function effectively as an edge-bridging group, because one component of the *e* set of its frontier molecular orbitals is not effectively utilized in bonding when it adopts such a position.[4]

The above arguments suggest that, relative to the $Au(PR_3)$ fragment, the $Cu(PR_3)$ moiety should show a preference for a face-bridging bonding mode in a mixed-metal cluster rather than an edge-bridging position. We were interested in experimentally testing these theoretical predictions by synthesizing several series of analogous heteronuclear clusters containing $M(PR_3)$ (M = Cu, Ag, or Au) fragments and examining the similarities and differences in the structures adopted by the different Group 1B metal congeners.

During the course of the work described herein, a number of reports[5–16] have appeared describing mixed-metal clusters containing one or more ML (M = Cu or Ag, L = two-electron donor ligand) units, although examples of this type of compound are still relatively rare, but discussion of any related work is deferred until later so that it can take place in the context of our results. Preliminary accounts describing some of our work have already been published.[17,18]

Results and Discussion

Copper and Silver Heteronuclear Clusters synthesized from the Salt $[N(PPh_3)_2][Ru_4(\mu\text{-}H)_3(CO)_{12}]$.—Treatment of a dichloromethane solution of the salt $[N(PPh_3)_2][Ru_4(\mu\text{-}H)_3(CO)_{12}]$ with one equivalent of the complex $[M(NCMe)_4]PF_6$ (M = Cu or Ag) at −30 °C incorporates a M(NCMe) unit into the cluster anion and subsequent addition of the requisite amount of the desired phosphine affords the dark orange cluster compounds $[MRu_4(\mu_3\text{-}H)_3(CO)_{12}L]$ [M = Cu, L = $PMePh_2$ (**1**) or PPh_3 (**2**); M = Ag, L = PPh_3 (**3**)] and $[\{MRu_4(\mu_3\text{-}H)_3(CO)_{12}\}_2(\mu\text{-}Ph_2PCH_2CH_2PPh_2)]$ [M = Cu (**6**) or Ag (**7**)] in *ca.* 70—80% yield. The intermediate species $[MRu_4(\mu_3\text{-}H)_3(CO)_{12}(NCMe)]$ [M = Cu (**4**) or Ag (**5**)] are too unstable to isolate as pure compounds, but the lability of their MeCN groups can be readily utilized for *in situ* ligand exchange reactions.[18] Alternatively, compounds (**2**) and (**3**) can also be prepared, in slightly reduced yield (*ca.* 60—70%), from the reacton of $[N(PPh_3)_2][Ru_4(\mu\text{-}H)_3(CO)_{12}]$ with one equivalent of the complex $[MX(PPh_3)]$ (M = Cu, X = Cl; M = Ag, X = I) in CH_2Cl_2 in the presence of $TlPF_6$.

The clusters (**1**)—(**3**), (**6**), and (**7**) were characterized by microanalyses and by spectroscopic measurements (Tables 1, 2, and 3). There are close similarities between the i.r. spectra of all these clusters and the ^1H n.m.r. spectrum of each compound at low temperature shows a single hydrido ligand resonance at high field, split by ^{31}P–^1H coupling and, in the case of (**3**) and (**7**), further complicated by $^{107,109}Ag$–^1H coupling. The $^{31}P\text{-}\{^1H\}$ n.m.r. spectra at −90 °C for (**1**)—(**3**), (**6**), and (**7**) show a signal due to a single phosphorus environment in each case, with additional splitting due to $^{107,109}Ag$–^{31}P coupling visible in the spectra of (**3**) and (**7**). At ambient temperature, the

Table 1. Analytical[a] and physical data for the Group 1B metal heteronuclear cluster compounds

Compound	M.p./°C (decomp.)	$\nu_{max.}$(CO)[b]/cm^{-1}	Yield (%)[c]	Analysis (%) C	H
(1) $[CuRu_4(\mu_3\text{-}H)_3(CO)_{12}(PMePh_2)]$	127—130	2 089m, 2 052vs, 2 029vs, 2 010m, 1 992s, 1 983m, 1 964w, 1 937vw	79	29.5 (29.8)	1.8 (1.6)
(2) $[CuRu_4(\mu_3\text{-}H)_3(CO)_{12}(PPh_3)]$	156—159	2 087m, 2 050vs, 2 025vs, 2 007m, 1 995s, 1 987m, 1 965w, 1 947vw	77	33.4 (33.7)	1.7 (1.7)
(3) $[AgRu_4(\mu_3\text{-}H)_3(CO)_{12}(PPh_3)]$	119—123	2 086m, 2 060s, 2 049vs, 2 023vs, 2 006s, 1 996(sh), 1 989s, 1 980(sh), 1 962w, 1 945w	69	32.3 (32.3)	1.6 (1.6)
(4) $[CuRu_4(\mu_3\text{-}H)_3(CO)_{12}(NCMe)]$[d]		[e] 2 088w, 2 051vs, 2 023s, 1 997m br			
(6) $[\{CuRu_4(\mu_3\text{-}H)_3(CO)_{12}\}_2(\mu\text{-}Ph_2PCH_2CH_2PPh_2)]$	179—183	[e] 2 089w, 2 054vs, 2 025s, 2 009m, 1 992m br	71	29.8 (29.8)	1.6 (1.5)
(7) $[\{AgRu_4(\mu_3\text{-}H)_3(CO)_{12}\}_2(\mu\text{-}Ph_2PCH_2CH_2PPh_2)]$	97—100	[e] 2 088w, 2 051vs, 2 022s, 2 007(sh), 1 986m br	70	28.6 (28.6)	1.3 (1.4)
(8) $[AuRu_4(\mu\text{-}H)_3(CO)_{12}(PPh_3)]$	145—147	2 089m, 2 062vs, 2 049s, 2 035(sh), 2 029vs, 2 012m, 2 003(sh), 1 999m, 1 978w br, 1 968w, 1 956vw	70	29.9 (30.0)	1.7 (1.5)
(9) $[\{AuRu_4(\mu\text{-}H)_3(CO)_{12}\}_2(\mu\text{-}Ph_2PCH_2PPh_2)]$	135—139	[e] 2 092m, 2 066vs, 2 050s, 2 030vs, 2 014(sh), 1 973m vbr	58	26.3 (26.0)	1.1 (1.2)
$[AuOs_4(\mu\text{-}H)_3(CO)_{12}(PEt_3)]$		[f] 2 094w, 2 071m, 2 038s, 2 033s, 2 009m, 2 001w, 1 994w, 1 976w, 1 967(sh), 1 948m			
(10) $[CuRu_3(CO)_9(C_2Bu^t)(PPh_3)]$	150—154	2 070m, 2 032vs, 1 990s br, 1 983(sh), 1 947m br	74	40.9 (41.2)	2.5 (2.5)
		[g] 2 066m, 2 026vs br, 1 992vs br, 1 976vs, 1 970(sh), 1 959s, 1 950vs, 1 937vs br, 1 911w, 1 896vw			
(11) $[AgRu_3(CO)_9(C_2Bu^t)(PPh_3)]$	163—166	2 069m, 2 029vs, 1 991s br, 1 977m, 1 953m br	67	39.3 (39.4)	2.3 (2.4)
		[g] 2 065m, 2 025vs br, 1 986vs br, 1 971vs br, 1 963(sh), 1 956s, 1 943vs br, 1 918w, 1 905vw			
(12) $[CuRu_3(CO)_9(C_2Bu^t)(NCMe)]$[d]		[e] 2 076w br, 2 046vs, 2 000m vbr, 1 966(sh)			
(13) $[AgRu_3(CO)_9(C_2Bu^t)(NCMe)]$[d]		[e] 2 080w br, 2 050vs br, 2 000m vbr			
(14) $[AuRu_3(CO)_9(C_2Bu^t)(PPh_3)]$[h]		[g] 2 072w, 2 032vs br, 2 009s, 1 994s, 1 988vs, 1 981vs, 1 974(sh), 1 965s, 1 960s, 1 950s, 1 928w			
(15) $[CuFe_3(\mu\text{-}COMe)(CO)_{10}(PPh_3)]$[i]		2 068m, 2 014vs, 1 997m, 1 991(sh), 1 978(sh), 1 969m br, 1 945w	44	43.6 (44.1)	1.9 (2.2)
(16) $[AgFe_3(\mu\text{-}COMe)(CO)_{10}(PPh_3)]$[d]		2 068m, 2 013vs, 1 996m, 1 990(sh), 1 979(sh), 1 971m br, 1 946w			

[a] Calculated values are given in parentheses. [b] Measured in cyclohexane solution, unless otherwise stated. [c] Based on ruthenium or iron reactant. When two alternative routes to the cluster exist, the best yield is quoted. [d] Cluster cannot be isolated as a pure compound. [e] Measured in dichloromethane solution. [f] Data from ref. 22; spectrum measured in hexane solution. [g] Measured as a suspension in Nujol mull. [h] Solution i.r. data given in ref. 25. [i] Compound slowly decomposes at room temperature.

$^{13}C\text{-}\{^1H\}$ n.m.r. resonances for the CO groups of (**1**) and (**6**) appear as sharp singlets and that of (**2**) as a sharp doublet [J(PC) 1 Hz], implying that all three clusters are undergoing dynamic behaviour involving CO site-exchange in solution. However, the spectra of the ground states of (**1**), (**2**), and (**6**) can be obtained at −90 °C and, for each cluster, the CO peaks then appear as three sharp singlets [relative intensity (r.i.) 1:2:1]. Thus, the spectroscopic data imply that (**1**)—(**3**), (**6**), and (**7**) have the same basic metal-core structure, with C_{3v} symmetry, and that all the hydrido ligands are equivalent and are bonded to the coinage metal as well as to ruthenium. Obviously, in the case of (**6**) and (**7**), two such structural units are linked together by the bidentate phosphine ligand. Furthermore, the close similarity between the values of J(PH) and J(AgH) for (**1**)—(**3**), (**6**), and (**7**) and those reported[5] for the triply-bridging hydrido ligands in $[MM'Ru_4(\mu_3\text{-}H)_2(CO)_{12}(PPh_3)_2]$ (M = M′ = Cu, Ag, or Au; M = Cu, M′ = Ag or Au; M = Ag, M′ = Au) suggests that the hydrido ligand bonding mode is the same for all of these clusters. To investigate the detailed molecular structure of a representative example from this interesting series, a single-crystal X-ray diffraction study was performed on cluster (**1**).

X-Ray crystal structure of $[CuRu_4(\mu_3\text{-}H)_3(CO)_{12}(PMePh_2)]$ (**1**). The molecular configuration of cluster (**1**) is shown in Figure 1, together with the crystallographic numbering, and the internuclear distances and angles are summarized in Table 4. The X-ray diffraction analysis confirms that the structure deduced by spectroscopic methods is correct. The metal core consists of a tetrahedron of ruthenium atoms with one of the triangular Ru_3 faces [Ru(1)Ru(2)Ru(3)] capped by a triply-bridging Cu($PMePh_2$) moiety to give a trigonal-bipyramidal geometry. Two of the three Cu–Ru distances, Cu–Ru(2) and Cu–Ru(3) [2.749(1) and 2.748(1) Å], are almost identical, but the third, Cu–Ru(1), is significantly shorter [2.717(1) Å], perhaps due to crystal packing effects from the asymmetrical phosphine ligand. All of the Cu–Ru distances lie in the previously observed range for Cu–Ru separations in heteronuclear clusters [2.577—2.809 Å].[5,9,10] As might be expected,[5,10] the

Table 2. Hydrogen-1 and phosphorus-31 n.m.r. data[a] for some selected Groub 1B metal heteronuclear cluster compounds

Compd.	^1H[b]	^{31}P[c]
(1)	[d] −17.56 (s, br, 3 H, μ_3-H), 2.01 [d, 3 H, PCH_3, J(PH) 7], 7.51—7.56 (m, 10 H, Ph)	−5.5 (s)
(2)	−17.58 [d, 3 H, μ_3-H, J(PH) 12], 7.43—7.54 (m, 15 H, Ph)	10.9 (s)
(3)	[e] −17.31 [2 × d of d, 3 H, μ_3-H, $J(^{109}AgH)$ 35, $J(^{107}AgH)$ 31, J(PH) 11], 7.36—7.60 (m, 15 H, Ph)	22.0 [2 × d, $J(^{109}AgP)$ 693, $J(^{107}AgP)$ 601]
(6)	[f] −17.70 [AA'X pattern, μ_3-H, 6 H, N(PH) 12], 2.55 (s, 4 H, PCH_2CH_2P), 7.42—7.58 (m, 20 H, Ph)	8.7 (s)
(7)	[f,g] −17.39 [2 × d of d, 6 H, μ_3-H, $J(^{109}AgH)$ 33, $J(^{107}AgH)$ 29, N(PH) 10], 1.60—3.05 (m, vbr, 4 H, PCH_2CH_2P), 7.19—7.67 (m, 20 H, Ph)	17.9 [m, $^1J(^{109}AgP)$ 690, $^1J(^{107}AgP)$ 598, ^3J(PP) 59, $^4J(^{107,109}AgP)$ 0, $^5J(^{107,109}Ag^{107,109}Ag)$ 0]
(8)	[h] −17.63 (s, 3 H, μ-H), 7.51—7.56 (m, 15 H, Ph)	[i]67.3 (s)
(9)	[j] −17.76 (s, 6 H, μ-H), 4.92 [t, 2 H, PCH_2P, J(PH) 8], 7.34—7.60 (m, 20 H, Ph)	[i]61.0 (s)
(10)	1.39 (s, 9 H, Bu^t), 7.35—7.47 (m, 15 H, Ph)	−1.4 (s)
(11)	1.40 (s, 9 H, Bu^t), 7.42—7.54 (m, 15 H, Ph)	12.2 [2 × d, $J(^{109}AgP)$ 482, $J(^{107}AgP)$ 417]
(14)	[k]1.37 (s, 9 H, Bu^t), 7.36—7.58 (m, 15 H, Ph)	[i,k]62.2 (s)
(15)	[k,l]4.31 (s, 3 H, OMe), 7.49 (s, br, 15 H, Ph)	[k,l]1.0 (s, br)
(16)	[k,m]4.35 (s, 3 H, OMe), 7.08—7.49 (m, 15 H, Ph)	

[a] Chemical shifts in p.p.m., coupling constants in Hz. [b] Measured in $[^2H_2]$dichloromethane at ambient temperature, unless otherwise stated. [c] Hydrogen-1 decoupled, measured in $[^2H_2]$dichloromethane at −90 °C, unless otherwise stated, chemical shifts positive to high frequency of 85% H_3PO_4 (external). [d] μ_3-H at −30 °C, δ −17.67 [d, 3 H, J(PH) 12]. [e] Measured at −80 °C; μ_3-H at ambient temperature, δ −17.21 (s, 3 H). [f] N(PH) = |J(PH) + J(P'H)|. [g] Measured at −50 °C. [h] μ-H at −90 °C, δ −18 (s, vbr, 3 H). [i] Measured at ambient temperature. [j] μ-H at −90 °C, δ −18.5 (s, vbr, 6 H). [k] Measured in $[^2H_1]$chloroform solution. [l] Measured at −30 °C. [m] Measured at −40 °C.

three unbridged Ru–Ru separations in the Ru_4 tetrahedron [Ru(1)–Ru(4) 2.789(1), Ru(2)–Ru(4) 2.788(1), Ru(3)–Ru(4) 2.797(1), mean 2.791(1) Å] are *ca.* 0.18 Å shorter than the three Ru–Ru edges bridged by the $Cu(PMePh_2)$ unit and the hydrido ligands [Ru(1)–Ru(2) 2.969(1), Ru(1)–Ru(3) 2.960(1), Ru(2)–Ru(3) 2.970(1), mean 2.966(1) Å]. Again, the symmetry of the molecule is distorted, so that, for each type of Ru–Ru vector, two of the separations are almost identical and the third is significantly different. All three $CuRu_2$ faces of the trigonal-bipyramidal metal core are capped by a triply-bridging hydrido ligand [mean Cu–H 1.93(6), mean Ru–H 1.81(6) Å]. Each ruthenium atom carries three CO ligands, which are essentially terminal, although the three nearest to the capping $Cu(PMePh_2)$ group and the hydrido ligands [CO(11), CO(21), and CO(31)] are bent more (mean Ru–C–O 173.7°) than the others (mean Ru–C–O 177.1°), presumably because of steric effects. The Cu–P distance [2.197(2) Å] is slightly shorter than the range previously observed in copper clusters [2.202—2.266 Å].[5,8,19]

There is a very close similarity between the structure observed for (1) and the capped trigonal-bipyramidal geometries adopted

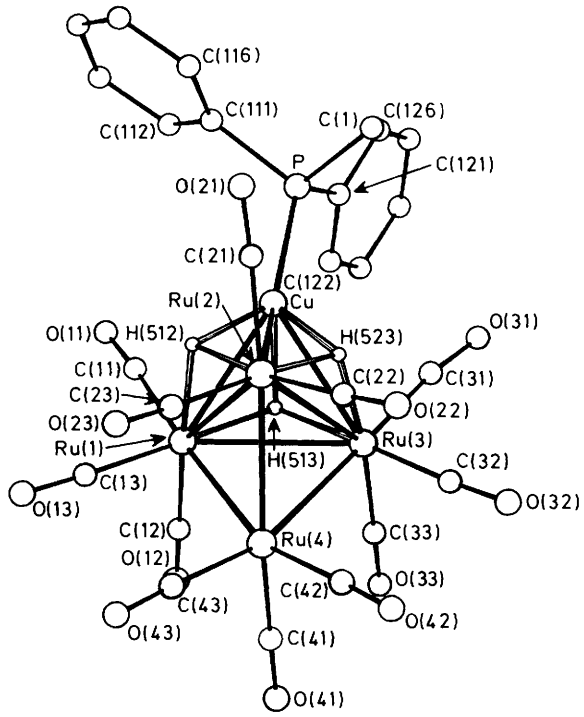

Figure 1. Molecular structure of $[CuRu_4(\mu_3\text{-}H)_3(CO)_{12}(PMePh_2)]$ (1), showing the crystallographic numbering scheme

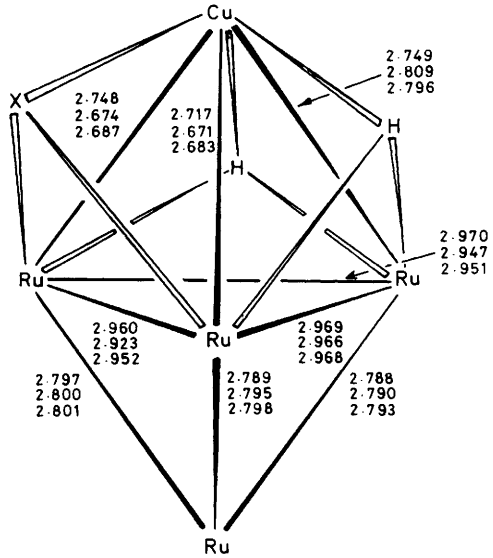

Figure 2. A comparison of the metal–metal separations (Å) within the basic $CuRu_4$ trigonal-bipyramidal structure common to $[CuRu_4(\mu_3\text{-}H)_3(CO)_{12}(PMePh_2)]$ (1) and $[CuMRu_4(\mu_3\text{-}H)_2(CO)_{12}(PPh_3)_2]$ (M = Cu or Ag). Distances are given first for (1), then for the Cu_2Ru_4 species, and finally for the $CuAgRu_4$ cluster; X = H, $Cu(PPh_3)$, or $Ag(PPh_3)$

by the hexanuclear clusters $[CuMRu_4(\mu_3\text{-}H)_2(CO)_{12}(PPh_3)_2]$[5] (M = Cu or Ag), with a triply-bridging hydrido ligand in the former replaced by a capping $M(PPh_3)$ fragment in the latter two species. Figure 2 compares the core structures of the three clusters in detail, illustrating the distortions which occur to the common $CuRu_4$ trigonal-bipyramidal unit when one of its $CuRu_2$ faces is capped by the various different groups X

Table 3. Carbon-13 n.m.r. data[a] for some selected Group 1B metal heteronuclear cluster compounds

Compd.	Full $^{13}C-\{^1H\}$ spectrum[b]	CO signals at low temperature[c]
(1)	195.2 (CO), 132.6 [d, C^2 (Ph), J(PC) 14], 131.9 [d, C^1 (Ph), J(PC) 43], 131.5 [d, C^4 (Ph), J(PC) 2], 129.7 [d, C^3 (Ph), J(PC) 10], 12.6 [d, PCH_3, J(PC) 27]	197.2 (3 CO), 196.6 (6 CO), 191.7 (3 CO)
(2)	195.2 [d, CO, J(PC) 1], 134.1 [d, C^2 (Ph), J(PC) 14], 131.7 [d, C^4 (Ph), J(PC) 2], 129.9 [d, C^1 (Ph), J(PC) 44], 129.8 [d, C^3 (Ph), J(PC) 11]	197.1 (3 CO), 196.6 (6 CO), 191.4 (3 CO)
(3)	[d] 196.6—195.1 (m, br, CO), 191.3 (br, CO), 134.1—128.7 (m, Ph)	
(6)	[e] 195.2 (CO), 133.1 [AA'X pattern, C^2 (Ph), N(PC) 14], 132.2 [C^4 (Ph)], 130.0 [AA'X pattern, C^3 (Ph), N(PC) 10], 129.3 [AA'X pattern, C^1 (Ph), N(PC) 42], 23.4 [AA'X pattern, PCH_2CH_2P, N(PC) 29]	196.9 (3 CO), 196.2 (6 CO), 192.4 (3 CO)
(8)	195.7 (CO), 134.3 [d, C^2 (Ph), J(PC) 15], 131.9 [d, C^1 (Ph), J(PC) 48], 131.7 [C^4 (Ph)], 129.5 [d, C^3 (Ph), J(PC) 11]	195.8
(10)	198.9—193.7 (m, br, CO), 174.9 ($CCBu^t$), 133.9 [d, C^2 (Ph), J(PC) 14], 131.3 [C^4 (Ph)], 130.0 [d, C^1 (Ph), J(PC) 40], 129.4 [d, C^3 (Ph), J(PC) 10], 121.4 ($CCBu^t$), 36.4 [$C(CH_3)_3$], 34.5 [$C(CH_3)_3$]	[f] 201.6 (br, 2 CO), 201.4 (1 CO), 194.3 (2 CO), 193.7 (2 CO), 189.5 [d, 2 CO, J(PC) 6]
(11)	199.8—194.4 (m, vbr, CO), 173.0 ($CCBu^t$), 133.8 [d, C^2 (Ph), J(PC) 16], 131.3 [C^4 (Ph)], 130.2 [d, C^1 (Ph), J(PC) 35], 129.4 [d, C^3 (Ph), J(PC) 10], 118.9 ($CCBu^t$), 36.2 [$C(CH_3)_3$], 34.5 [$C(CH_3)_3$]	[f] 201.9 (br, 3 CO), 195.5 (2 CO), 193.3 (2 CO), 189.8 (br, 2 CO)
(14)	197 (vbr, CO), 172.2 ($CCBu^t$), 134.3 [d, C^2 (Ph), J(PC) 15], 131.7 [d, C^4 (Ph), J(PC) 2], 131.6 [d, C^1 (Ph), J(PC) 49], 129.5 [d, C^3 (Ph), J(PC) 11], 120.7 ($CCBu^t$), 36.5 [$C(CH_3)_3$], 34.7 [$C(CH_3)_3$]	204.3 (br, 2 CO), 203.0 (1 CO), 196.8 (2 CO), 195.0 (2 CO), 194.0 [d, 2 CO, J(PC) 13]
(15)	[g] 333.7 (μ-COMe), 214.1 (CO), 133.9 [d, C^2 (Ph), J(PC) 15], 131.6 [C^4 (Ph)], 129.6 [d, C^1 (Ph), J(PC) 42], 129.6 [d, C^3 (Ph), J(PC) 10], 71.1 (μ-$COCH_3$)	211.0 (br)

[a] Hydrogen-1 decoupled, chemical shifts (δ) in p.p.m., with positive values of δ representing shifts to high frequency of $SiMe_4$, coupling constants in Hz, measured in $[^2H_2]$dichloromethane–CH_2Cl_2 solution. [b] Measured at ambient temperature, unless otherwise stated. [c] Measured at −90 °C, unless otherwise stated. [d] Measured at −90 °C. [e] N(PC) = |J(PC) + J(P'C)|. [f] Measured at −100 °C. [g] Measured at −30 °C.

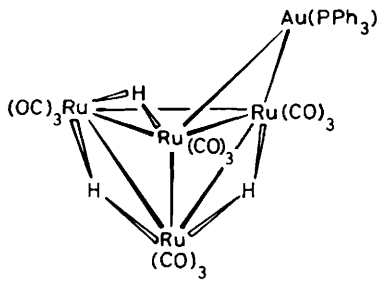

(8)

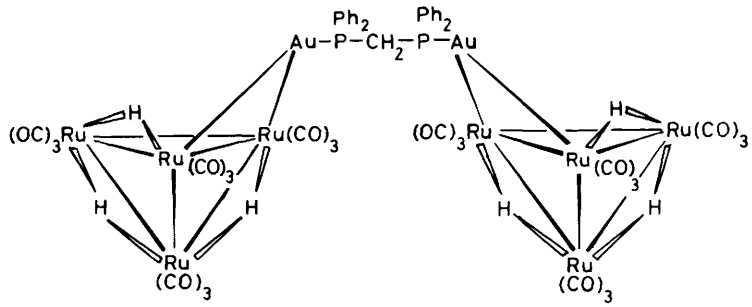

(9)

[X = H, Cu(PPh_3), or Ag(PPh_3)]. As might be expected, the unbridged Ru–Ru separations change little with X, but the Ru–Ru and the two Cu–Ru distances in the $CuRu_2$ face capped by X are quite significantly larger when X = H than when X = M(PPh_3) (M = Cu or Ag). Correspondingly, the third Cu–Ru separation is significantly smaller when X = H than when X = M(PPh_3).

Gold Heteronuclear Clusters synthesized from the Salt $[N(PPh_3)_2][Ru_4(\mu\text{-}H)_3(CO)_{12}]$.—The analogous gold species $[AuRu_4(\mu\text{-}H)_3(CO)_{12}(PPh_3)]$ (**8**) (70% yield) and $[\{AuRu_4(\mu\text{-}H)_3(CO)_{12}\}_2(\mu\text{-}Ph_2PCH_2PPh_2)]$ (**9**) (58% yield), also dark orange, can be readily prepared by treating a CH_2Cl_2 solution of $[N(PPh_3)_2][Ru_4(\mu\text{-}H)_3(CO)_{12}]$ with one equivalent of $[AuCl(PPh_3)]$ or half an equivalent of $[Au_2(\mu\text{-}Ph_2PCH_2PPh_2)Cl_2]$, respectively, in the presence of $TlPF_6$. The preparation of (**9**) also produces a small amount (10% yield) of the known hexanuclear cluster $[Au_2Ru_4(\mu_3\text{-}H)(\mu\text{-}H)(\mu\text{-}Ph_2PCH_2PPh_2)(CO)_{12}]$.[20] The i.r. spectra of (**8**) and (**9**) (Table 1) are closely similar, but they show a somewhat different pattern of bands to those of (**1**)—(**3**), (**6**), and (**7**), implying that (**8**) and (**9**) have common metal-core structures, but that this geometry is different from that adopted by (**1**)—(**3**), (**6**), and (**7**). Hydrogen-1 n.m.r. spectra of (**8**) and (**9**) (Table 2) each show a hydrido ligand resonance at high field, but the signals are singlets and the absence of $^{31}P-^1H$ coupling suggests that the hydrido ligands do not cap $AuRu_2$ faces in these clusters. Lewis and co-workers[21] have prepared a gold–osmium cluster $[AuOs_4(\mu\text{-}H)_3(CO)_{12}(PEt_3)]$ analogous to (**8**) and established its structure by a single-crystal *X*-ray diffraction study. The $Au(PEt_3)$ moiety bridges one edge of an Os_4 tetrahedron, with three other edges of this osmium core bridged by hydrido ligands. In view of the very close similarity between the i.r. (Table 1) and ^1H n.m.r. (the hydrido ligand signal is a singlet at

Table 4. Selected bond lengths (Å) and angles (°), with estimated standard deviations in parentheses, for $[CuRu_4(\mu_3\text{-}H)_3(CO)_{12}(PMePh_2)]$ (**1**)

Ru(1)–Ru(2)	2.969(1)	Ru(1)–Ru(3)	2.960(1)	Ru(4)–C(41)	1.889(7)	Ru(4)–C(42)	1.898(7)
Ru(1)–Ru(4)	2.789(1)	Ru(1)–Cu	2.717(1)	Ru(4)–C(43)	1.874(7)	Cu–H(512)	1.91(6)
Ru(1)–H(512)	1.89(6)	Ru(1)–H(513)	1.80(6)	Cu–H(513)	1.96(6)	Cu–H(523)	1.92(6)
Ru(1)–C(11)	1.949(7)	Ru(1)–C(12)	1.906(7)	Cu–P	2.197(2)	P–C(1)	1.836(8)
Ru(1)–C(13)	1.900(7)	Ru(2)–Ru(3)	2.970(1)	P–C(111)	1.806(6)	P–C(121)	1.820(6)
Ru(2)–Ru(4)	2.788(1)	Ru(2)–Cu	2.749(1)	C(11)–O(11)	1.128(9)	C(12)–O(12)	1.119(10)
Ru(2)–H(512)	1.79(6)	Ru(2)–H(523)	1.78(6)	C(13)–O(13)	1.132(9)	C(21)–O(21)	1.123(9)
Ru(2)–C(21)	1.943(7)	Ru(2)–C(22)	1.887(7)	C(22)–O(22)	1.132(9)	C(23)–O(23)	1.138(10)
Ru(2)–C(23)	1.898(8)	Ru(3)–Ru(4)	2.797(1)	C(31)–O(31)	1.131(8)	C(32)–O(32)	1.122(10)
Ru(3)–Cu	2.748(1)	Ru(3)–H(513)	1.76(6)	C(33)–O(33)	1.141(10)	C(41)–O(41)	1.134(9)
Ru(3)–H(523)	1.81(6)	Ru(3)–C(31)	1.938(7)	C(42)–O(42)	1.130(9)	C(43)–O(43)	1.148(9)
Ru(3)–C(32)	1.891(8)	Ru(3)–C(33)	1.892(8)	C–C (phenyl)	1.38 (mean)		
Ru(3)–Ru(1)–Ru(2)	60.1(1)	Ru(4)–Ru(1)–Ru(2)	57.8(1)	C(31)–Ru(3)–Ru(2)	119.6(2)	C(31)–Ru(3)–Ru(4)	177.1(2)
Ru(4)–Ru(1)–Ru(3)	58.1(1)	Cu–Ru(1)–Ru(2)	57.6(1)	C(31)–Ru(3)–Cu	75.5(2)	C(31)–Ru(3)–H(513)	89(2)
Cu–Ru(1)–Ru(3)	57.7(1)	Cu–Ru(1)–Ru(4)	104.0(1)	C(31)–Ru(3)–H(523)	86(2)	C(32)–Ru(3)–Ru(1)	141.8(2)
H(512)–Ru(1)–Ru(2)	35(2)	H(512)–Ru(1)–Ru(3)	83(2)	C(32)–Ru(3)–Ru(2)	95.3(2)	C(32)–Ru(3)–Ru(4)	84.7(2)
H(512)–Ru(1)–Ru(4)	92(2)	H(512)–Ru(1)–Cu	45(2)	C(32)–Ru(3)–Cu	136.4(2)	C(32)–Ru(3)–H(513)	176(2)
H(513)–Ru(1)–Ru(2)	82(2)	H(513)–Ru(1)–Ru(3)	33(2)	C(32)–Ru(3)–H(523)	94(2)	C(32)–Ru(3)–C(31)	94.6(3)
H(513)–Ru(1)–Ru(4)	91(2)	H(513)–Ru(1)–Cu	46(2)	C(33)–Ru(3)–Ru(1)	93.3(2)	C(33)–Ru(3)–Ru(2)	142.6(2)
H(513)–Ru(1)–H(512)	88(3)	C(11)–Ru(1)–Ru(2)	119.1(2)	C(33)–Ru(3)–Ru(4)	86.5(2)	C(33)–Ru(3)–Cu	131.6(2)
C(11)–Ru(1)–Ru(3)	119.1(2)	C(11)–Ru(1)–Ru(4)	176.4(2)	C(33)–Ru(3)–H(513)	88(2)	C(33)–Ru(3)–H(523)	174(2)
C(11)–Ru(1)–Cu	72.4(2)	C(11)–Ru(1)–H(512)	85(2)	C(33)–Ru(3)–C(31)	96.4(3)	C(33)–Ru(3)–C(32)	91.2(3)
C(11)–Ru(1)–H(513)	87(2)	C(12)–Ru(1)–Ru(2)	144.2(2)	Ru(2)–Ru(4)–Ru(1)	64.3(1)	Ru(3)–Ru(4)–Ru(1)	64.0(1)
C(12)–Ru(1)–Ru(3)	94.8(2)	C(12)–Ru(1)–Ru(4)	87.8(2)	Ru(3)–Ru(4)–Ru(2)	64.2(1)	C(41)–Ru(4)–Ru(1)	100.5(2)
C(12)–Ru(1)–Cu	132.7(2)	C(12)–Ru(1)–H(512)	177(2)	C(41)–Ru(4)–Ru(2)	160.2(2)	C(41)–Ru(4)–Ru(3)	98.3(2)
C(12)–Ru(1)–H(513)	89(2)	C(12)–Ru(1)–C(11)	94.9(3)	C(42)–Ru(4)–Ru(1)	160.3(2)	C(42)–Ru(4)–Ru(2)	99.2(2)
C(13)–Ru(1)–Ru(2)	94.4(2)	C(13)–Ru(1)–Ru(3)	141.7(2)	C(42)–Ru(4)–Ru(3)	99.9(2)	C(42)–Ru(4)–C(41)	92.8(3)
C(13)–Ru(1)–Ru(4)	84.5(2)	C(13)–Ru(1)–Cu	134.6(2)	C(43)–Ru(4)–Ru(1)	102.0(2)	C(43)–Ru(4)–Ru(2)	102.5(2)
C(13)–Ru(1)–H(512)	91(2)	C(13)–Ru(1)–H(513)	175(2)	C(43)–Ru(4)–Ru(3)	163.5(2)	C(43)–Ru(4)–C(41)	92.7(3)
C(13)–Ru(1)–C(11)	97.9(3)	C(13)–Ru(1)–C(12)	91.6(3)	C(43)–Ru(4)–C(42)	91.7(3)	Ru(2)–Cu–Ru(1)	65.8(1)
Ru(3)–Ru(2)–Ru(1)	59.8(1)	Ru(4)–Ru(2)–Ru(1)	57.9(1)	Ru(3)–Cu–Ru(1)	65.6(1)	Ru(3)–Cu–Ru(2)	65.4(1)
Ru(4)–Ru(2)–Ru(3)	58.0(1)	Cu–Ru(2)–Ru(1)	56.6(1)	H(512)–Cu–Ru(1)	44(2)	H(512)–Cu–Ru(2)	40(2)
Cu–Ru(2)–Ru(3)	57.3(1)	Cu–Ru(2)–Ru(4)	103.2(1)	H(512)–Cu–Ru(3)	88(2)	H(513)–Cu–Ru(1)	41(2)
H(512)–Ru(2)–Ru(1)	37(2)	H(512)–Ru(2)–Ru(3)	84(2)	H(513)–Cu–Ru(2)	86(2)	H(513)–Cu–Ru(3)	40(2)
H(512)–Ru(2)–Ru(4)	94(2)	H(512)–Ru(2)–Cu	44(2)	H(513)–Cu–H(512)	83(2)	H(523)–Cu–Ru(1)	86(2)
H(523)–Ru(2)–Ru(1)	81(2)	H(523)–Ru(2)–Ru(3)	35(2)	H(523)–Cu–Ru(2)	40(2)	H(523)–Cu–Ru(3)	41(2)
H(523)–Ru(2)–Ru(4)	92(2)	H(523)–Ru(2)–Cu	44(2)	H(523)–Cu–H(512)	79(2)	H(523)–Cu–H(513)	79(2)
H(523)–Ru(2)–H(512)	86(3)	C(21)–Ru(2)–Ru(1)	117.8(2)	P–Cu–Ru(1)	148.9(1)	P–Cu–Ru(2)	139.1(1)
C(21)–Ru(2)–Ru(3)	123.2(2)	C(21)–Ru(2)–Ru(4)	174.9(2)	P–Cu–Ru(3)	134.7(1)	P–Cu–H(512)	136(2)
C(21)–Ru(2)–Cu	74.9(2)	C(21)–Ru(2)–H(512)	81(2)	P–Cu–H(513)	133(2)	P–Cu–H(523)	125(2)
C(21)–Ru(2)–H(523)	90(2)	C(22)–Ru(2)–Ru(1)	143.8(2)	Ru(2)–H(512)–Ru(1)	108(3)	Cu–H(512)–Ru(1)	91(3)
C(22)–Ru(2)–Ru(3)	93.3(2)	C(22)–Ru(2)–Ru(4)	88.0(2)	Cu–H(512)–Ru(2)	96(3)	Ru(3)–H(513)–Ru(1)	112(3)
C(22)–Ru(2)–Cu	131.2(2)	C(22)–Ru(2)–H(512)	175(2)	Cu–H(513)–Ru(1)	92(3)	Cu–H(513)–Ru(3)	95(3)
C(22)–Ru(2)–H(523)	89(2)	C(22)–Ru(2)–C(21)	96.8(3)	Ru(3)–H(523)–Ru(2)	111(3)	Cu–H(523)–Ru(2)	96(3)
C(23)–Ru(2)–Ru(1)	94.3(2)	C(23)–Ru(2)–Ru(3)	139.2(2)	Cu–H(523)–Ru(3)	95(3)	C(1)–P–Cu	111.0(2)
C(23)–Ru(2)–Ru(4)	81.8(2)	C(23)–Ru(2)–Cu	136.1(2)	C(111)–P–Cu	117.0(2)	C(111)–P–C(1)	105.1(3)
C(23)–Ru(2)–H(512)	93(2)	C(23)–Ru(2)–H(523)	174(2)	C(121)–P–Cu	114.0(2)	C(121)–P–C(1)	104.8(3)
C(23)–Ru(2)–C(21)	96.1(3)	C(23)–Ru(2)–C(22)	92.1(3)	C(121)–P–C(111)	103.9(3)	O(11)–C(11)–Ru(1)	174.1(6)
Ru(2)–Ru(3)–Ru(1)	60.1(1)	Ru(4)–Ru(3)–Ru(1)	57.9(1)	O(12)–C(12)–Ru(1)	176.9(7)	O(13)–C(13)–Ru(1)	177.9(7)
Ru(4)–Ru(3)–Ru(2)	57.7(1)	Cu–Ru(3)–Ru(1)	56.7(1)	O(21)–C(21)–Ru(2)	174.7(7)	O(22)–C(22)–Ru(2)	177.1(7)
Cu–Ru(3)–Ru(2)	57.3(1)	Cu–Ru(3)–Ru(4)	103.0(1)	O(23)–C(23)–Ru(2)	176.4(7)	O(31)–C(31)–Ru(3)	172.2(6)
H(513)–Ru(3)–Ru(1)	34(2)	H(513)–Ru(3)–Ru(2)	83(2)	O(32)–C(32)–Ru(3)	176.2(7)	O(33)–C(33)–Ru(3)	177.5(7)
H(513)–Ru(3)–Ru(4)	91(2)	H(513)–Ru(3)–Cu	45(2)	O(41)–C(41)–Ru(4)	177.0(7)	O(42)–C(42)–Ru(4)	178.1(7)
H(523)–Ru(3)–Ru(1)	81(2)	H(523)–Ru(3)–Ru(2)	34(2)	O(43)–C(43)–Ru(4)	177.0(6)	C(112)–C(111)–P	120.9(6)
H(523)–Ru(3)–Ru(4)	91(2)	H(523)–Ru(3)–Cu	44(2)	C(116)–C(111)–P	120.5(5)	C(122)–C(121)–P	119.2(5)
H(523)–Ru(3)–H(513)	87(3)	C(31)–Ru(3)–Ru(1)	122.4(2)	C(126)–C(121)–P	121.3(5)		

δ −17.94 p.p.m., in $CDCl_3$[22]) data of the gold–osmium cluster and those for (**8**) and (**9**), it seems reasonable to postulate that (**8**) adopts the same structure as the former, and that the two pentanuclear metal units linked together by the bidentate phosphine in (**9**) also exhibit a similar geometry. The proposed structures for (**8**) and (**9**) are also reasonable, as they are closely related to that of the analogous hydrido complex $[Ru_4(\mu\text{-}H)_4(CO)_{12}]$,[23] with a hydrido ligand in the latter being replaced by an isolobal $Au(PR_3)$ group[3] in the former two species, (**8**) and (**9**). Clearly, the hydrido ligands are not all equivalent in the proposed solid-state structures of (**8**) and (**9**), although they only show singlet peaks in the room-temperature ^1H n.m.r. spectra. However, a very broad ^1H n.m.r. high-field resonance is observed for the hydrido ligands in (**8**) and (**9**) at −90 °C, consistent with both clusters undergoing a dynamic process at room temperature involving site-exchange of the hydrido ligands. While the work described herein was in progress, compound (**8**) was also obtained by Bruce and Nicholson[24] and the PEt_3 analogue of (**8**) has been very briefly reported by Lewis and co-workers.[21]

Thus, for the copper–ruthenium and silver–ruthenium clusters (**1**)—(**3**), (**6**), and (**7**), the $M(PR_3)$ (M = Cu or Ag) fragments cap a face of the tetrahedral ruthenium core, whereas in the analogous gold–ruthenium species (**8**) and (**9**), the $Au(PR_3)$

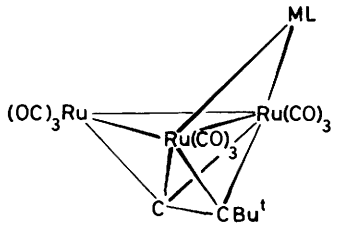

	M	L
(10)	Cu	PPh_3
(11)	Ag	PPh_3
(12)	Cu	NCMe
(13)	Ag	NCMe
(14)	Au	PPh_3

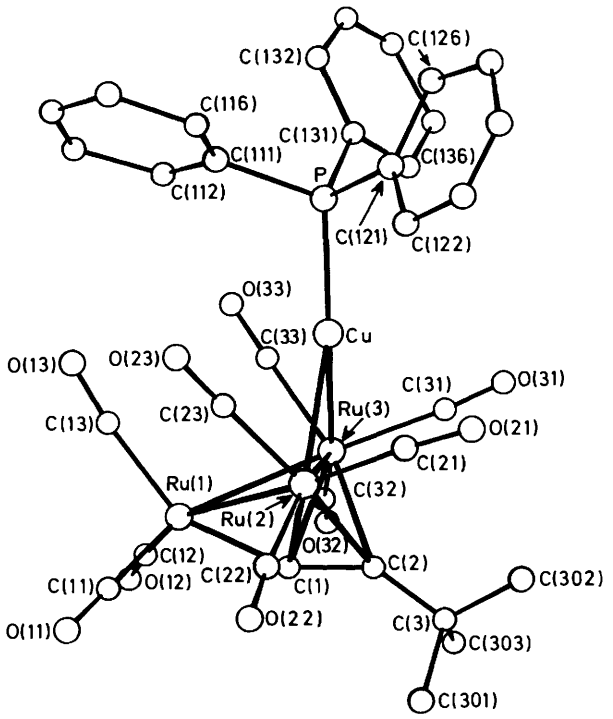

Figure 3. Molecular structure of $[CuRu_3(CO)_9(C_2Bu^t)(PPh_3)]$ (**10**), showing the crystallographic numbering scheme

moiety bridges one edge of the basic Ru_4 tetrahedron. A similar coinage metal site-preference has been recently reported[6] for the salts $[PMePh_3][MOs_{10}C(CO)_{24}L]$ (M = Cu, L = NCMe; M = Au, L = PPh_3). It is also interesting that a thermodynamic preference has been previously observed[5] for the lighter of the two Group 1B metals to occupy the hydrido ligand–capped sites, triply-bridging triangular Ru_3 faces, in the capped trigonal-bipyramidal metal cores of the trimetallic clusters $[MM'Ru_4(\mu_3\text{-}H)_2(CO)_{12}(PPh_3)_2]$ (M = Cu, M' = Ag or Au; M = Ag, M' = Au). These preferred positions for the lighter coinage metals are very similar to those taken up by the $M(PR_3)$ (M = Cu or Ag) fragments in (**1**)—(**3**), (**6**), and (**7**) (Figure 2).

Heteronuclear Group 1B *Metal Clusters synthesized from the Salt* $[N(PPh_3)_2][Ru_3(CO)_9(C_2Bu^t)]$.—In contrast to the numerous heteronuclear clusters containing a $Au(PR_3)$ unit bridging a metal-metal bond now known,[1] until very recently no well characterized examples of analogous copper and silver species had been reported. Thus, in an attempt to prepare such clusters for detailed study, we treated a dichloromethane

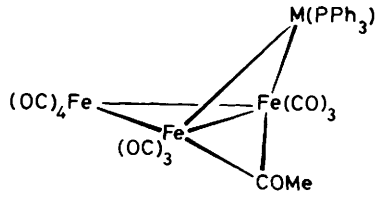

	M
(15)	Cu
(16)	Ag
(17)	Au

solution of the salt $[N(PPh_3)_2][Ru_3(CO)_9(C_2Bu^t)]$ with one equivalent of $[M(NCMe)_4]PF_6$ (M = Cu or Ag) at −30 °C, followed by the addition of one equivalent of PPh_3, to afford the yellow mixed-metal clusters $[MRu_3(CO)_9(C_2Bu^t)(PPh_3)]$ [M = Cu (**10**) or Ag (**11**)] (74 and 67% yield). Again, the intermediate species $[MRu_3(CO)_9(C_2Bu^t)(NCMe)]$ [M = Cu (**12**) or Ag (**13**)] are too unstable to isolate as pure compounds. Much reduced yields of (**10**) and (**11**) (*ca.* 40%) can also be obtained *via* the alternative route of treating a dichloromethane solution of $[N(PPh_3)_2][Ru_3(CO)_9(C_2Bu^t)]$ with $[MX(PPh_3)]$ (M = Cu, X = Cl; M = Ag, X = I), in the presence of $TlPF_6$.

The characteristic signals in the ^1H and $^{13}C\text{-}\{^1H\}$ n.m.r. spectra of (**10**) and (**11**) (Tables 2 and 3) show that the t-butylacetylide ligand has been retained in these clusters. A resonance due to a single phosphorus environment is observed in the $^{31}P\text{-}\{^1H\}$ n.m.r. spectrum of each cluster at −90 °C (Table 2), with additional splitting due to $^{107,109}Ag\text{–}^{31}P$ coupling visible in the spectrum of (**11**). At room temperature, the signals due to the CO ligands in the $^{13}C\text{-}\{^1H\}$ n.m.r. spectra of (**10**) and (**11**) are broad, indicating that these clusters are undergoing dynamic behaviour involving CO site-exchange in solution. However, static spectra can be obtained at −100 °C. Compound (**10**) shows five CO signals (r.i. 2:1:2:2:2), one of which is split into a doublet by $^{31}P\text{–}^{13}C$ coupling, whereas four CO peaks (r.i. 3:2:2:2) are visible for (**11**). Both of these patterns are fully consistent with (**10**) and (**11**) having the same 'butterfly' metal-core structure as that adopted by the analogous gold cluster $[AuRu_3(CO)_9(C_2Bu^t)(PPh_3)]$ (**14**).[25] However, in order to perform detailed structural comparisons between two members of this interesting series of clusters, a single-crystal *X*-ray diffraction study was undertaken on the copper–ruthenium species (**10**).

X-*Ray crystal structure of* $[CuRu_3(CO)_9(C_2Bu^t)(PPh_3)]$ (**10**). The molecular configuration of cluster (**10**) is shown in Figure 3, together with the crystallographic numbering scheme, and the internuclear distances and angles are summarized in Table 5. The *X*-ray diffraction analysis confirms that the structure deduced by spectroscopic methods is correct. The heteronuclear cluster can be envisaged as a molecule of $[Ru_3(\mu\text{-}H)(CO)_9(C_2Bu^t)]$[26] in which the bridging hydrido ligand is replaced by a bridging $Cu(PPh_3)$ unit, thus producing a 'butterfly' metal core, with the copper atom occupying a 'wing-tip' site. The interplanar angle between the two metal triangles is 115.7° in (**10**) compared to 129.3° in the analogous gold species (**14**).[25] The two Cu–Ru bond lengths are equal [2.603(1) Å] and lie in the observed range for Cu–Ru separations [2.557—2.809 Å].[5,9,10] The three ruthenium atoms define a triangle, with the Ru–Ru edge [2.762(1) Å] bridged by the $Cu(PPh_3)$ fragment being significantly shorter than the other two Ru–Ru distances [2.819(1) and 2.808(1) Å]. The Cu–P distance [2.217(2) Å] is unremarkable, lying in the range previously observed for copper clusters [2.202—2.266 Å].[5,8,19] The t-butylacetylide ligand lies on the convex side of the 'butterfly' metal core, interacting with

Table 5. Selected bond lengths (Å) and angles (°), with estimated standard deviations in parentheses, for $[CuRu_3(CO)_9(C_2Bu^t)(PPh_3)]$ (**10**)

Ru(1)–Ru(2)	2.819(1)	Ru(1)–Ru(3)	2.808(1)	Cu–C(33)	2.496(7)	Cu–P	2.217(2)
Ru(1)–C(1)	1.945(7)	Ru(1)–C(11)	1.877(9)	C(1)–C(2)	1.313(9)	C(2)–C(3)	1.506(9)
Ru(1)–C(12)	1.896(9)	Ru(1)–C(13)	1.931(9)	C(3)–C(301)	1.539(12)	C(3)–C(302)	1.540(11)
Ru(2)–Ru(3)	2.762(1)	Ru(2)–Cu	2.603(1)	C(3)–C(303)	1.527(12)	C(11)–O(11)	1.155(9)
Ru(2)–C(1)	2.203(6)	Ru(2)–C(2)	2.260(7)	C(12)–O(12)	1.118(9)	C(13)–O(13)	1.132(9)
Ru(2)–C(21)	1.927(8)	Ru(2)–C(22)	1.919(8)	C(21)–O(21)	1.127(8)	C(22)–O(22)	1.144(8)
Ru(2)–C(23)	1.900(9)	Ru(3)–Cu	2.603(1)	C(23)–O(23)	1.154(9)	C(31)–O(31)	1.140(8)
Ru(3)–C(1)	2.211(7)	Ru(3)–C(2)	2.259(6)	C(32)–O(32)	1.113(9)	C(33)–O(33)	1.149(8)
Ru(3)–C(31)	1.910(8)	Ru(3)–C(32)	1.927(9)	P–C(111)	1.827(8)	P–C(121)	1.802(8)
Ru(3)–C(33)	1.896(8)	Cu–C(23)	2.552(7)	P–C(131)	1.824(8)	C–C(phenyl)	1.38 (mean)
Ru(3)–Ru(1)–Ru(2)	58.8(1)	C(1)–Ru(1)–Ru(2)	51.2(2)	C(32)–Ru(3)–C(2)	100.4(3)	C(32)–Ru(3)–C(31)	96.0(4)
C(1)–Ru(1)–Ru(3)	51.6(2)	C(11)–Ru(1)–Ru(2)	100.4(3)	C(33)–Ru(3)–Ru(1)	86.2(2)	C(33)–Ru(3)–Ru(2)	109.4(2)
C(11)–Ru(1)–Ru(3)	155.4(3)	C(11)–Ru(1)–C(1)	105.9(3)	C(33)–Ru(3)–Cu	65.2(2)	C(33)–Ru(3)–C(1)	129.7(3)
C(12)–Ru(1)–Ru(2)	152.3(2)	C(12)–Ru(1)–Ru(3)	99.2(3)	C(33)–Ru(3)–C(2)	159.7(3)	C(33)–Ru(3)–C(31)	100.2(3)
C(12)–Ru(1)–C(1)	102.8(3)	C(12)–Ru(1)–C(11)	95.8(4)	C(33)–Ru(3)–C(32)	92.4(3)	Ru(3)–Cu–Ru(2)	64.1(1)
C(13)–Ru(1)–Ru(2)	103.7(2)	C(13)–Ru(1)–Ru(3)	102.2(2)	C(23)–Cu–Ru(2)	43.3(2)	C(23)–Cu–Ru(3)	97.3(2)
C(13)–Ru(1)–C(1)	149.2(3)	C(13)–Ru(1)–C(11)	95.2(4)	C(33)–Cu–Ru(2)	97.5(2)	C(33)–Cu–Ru(3)	43.6(2)
C(13)–Ru(1)–C(12)	97.0(3)	Ru(3)–Ru(2)–Ru(1)	60.4(1)	C(33)–Cu–C(23)	107.4(3)	P–Cu–Ru(2)	145.8(1)
Cu–Ru(2)–Ru(1)	93.3(1)	Cu–Ru(2)–Ru(3)	58.0(1)	P–Cu–Ru(3)	149.7(1)	P–Cu–C(23)	107.0(2)
C(1)–Ru(2)–Ru(1)	43.5(2)	C(1)–Ru(2)–Ru(3)	51.4(2)	P–Cu–C(33)	110.1(2)	Ru(2)–C(1)–Ru(1)	85.4(2)
C(1)–Ru(2)–Cu	108.5(2)	C(2)–Ru(2)–Ru(1)	76.7(2)	Ru(3)–C(1)–Ru(1)	84.7(2)	Ru(3)–C(1)–Ru(2)	77.5(2)
C(2)–Ru(2)–Ru(3)	52.3(2)	C(2)–Ru(2)–Cu	104.3(2)	C(2)–C(1)–Ru(1)	154.4(5)	C(2)–C(1)–Ru(2)	75.3(4)
C(2)–Ru(2)–C(1)	34.2(2)	C(21)–Ru(2)–Ru(1)	163.8(2)	C(2)–C(1)–Ru(3)	74.9(4)	Ru(3)–C(2)–Ru(2)	75.3(2)
C(21)–Ru(2)–Ru(3)	103.4(2)	C(21)–Ru(2)–Cu	76.2(2)	C(1)–C(2)–Ru(2)	70.5(4)	C(1)–C(2)–Ru(3)	70.9(4)
C(21)–Ru(2)–C(1)	127.9(3)	C(21)–Ru(2)–C(2)	93.7(3)	C(3)–C(2)–Ru(2)	135.6(5)	C(3)–C(2)–Ru(3)	135.9(5)
C(22)–Ru(2)–Ru(1)	97.1(2)	C(22)–Ru(2)–Ru(3)	144.8(2)	C(3)–C(2)–C(1)	139.9(7)	C(301)–C(3)–C(2)	107.3(7)
C(22)–Ru(2)–Cu	156.5(2)	C(22)–Ru(2)–C(1)	93.5(3)	C(302)–C(3)–C(2)	113.8(7)	C(302)–C(3)–C(301)	108.1(7)
C(22)–Ru(2)–C(2)	98.6(3)	C(22)–Ru(2)–C(21)	97.2(3)	C(303)–C(3)–C(2)	107.1(6)	C(303)–C(3)–C(301)	110.6(9)
C(23)–Ru(2)–Ru(1)	86.4(2)	C(23)–Ru(2)–Ru(3)	110.9(2)	C(303)–C(3)–C(302)	109.8(8)	O(11)–C(11)–Ru(1)	175.7(9)
C(23)–Ru(2)–Cu	66.9(2)	C(23)–Ru(2)–C(1)	129.9(3)	O(12)–C(12)–Ru(1)	175.5(8)	O(13)–C(13)–Ru(1)	175.9(8)
C(23)–Ru(2)–C(2)	160.6(3)	C(23)–Ru(2)–C(21)	100.4(3)	O(21)–C(21)–Ru(2)	177.7(7)	O(22)–C(22)–Ru(2)	178.1(7)
C(23)–Ru(2)–C(22)	92.7(3)	Ru(2)–Ru(3)–Ru(1)	60.8(1)	Cu–C(23)–Ru(2)	69.8(2)	O(23)–C(23)–Ru(2)	174.9(6)
Cu–Ru(3)–Ru(1)	93.6(1)	Cu–Ru(3)–Ru(2)	58.0(1)	O(23)–C(23)–Cu	115.0(5)	O(31)–C(31)–Ru(3)	176.9(8)
C(1)–Ru(3)–Ru(1)	43.6(2)	C(1)–Ru(3)–Ru(2)	51.1(2)	O(32)–C(32)–Ru(3)	178.0(8)	Cu–C(33)–Ru(3)	71.2(2)
C(1)–Ru(3)–Cu	108.2(2)	C(2)–Ru(3)–Ru(1)	76.9(2)	O(33)–C(33)–Ru(3)	176.1(7)	O(33)–C(33)–Cu	112.7(6)
C(2)–Ru(3)–Ru(2)	52.3(2)	C(2)–Ru(3)–Cu	104.3(2)	C(111)–P–Cu	111.4(2)	C(121)–P–Cu	114.0(3)
C(2)–Ru(3)–C(1)	34.2(2)	C(31)–Ru(3)–Ru(1)	165.9(2)	C(121)–P–C(111)	106.0(3)	C(131)–P–Cu	115.2(3)
C(31)–Ru(3)–Ru(2)	105.1(2)	C(31)–Ru(3)–Cu	78.0(2)	C(131)–P–C(111)	103.5(3)	C(131)–P–C(121)	105.8(3)
C(31)–Ru(3)–C(1)	128.2(3)	C(31)–Ru(3)–C(2)	94.0(3)	C(112)–C(111)–P	118.6(6)	C(116)–C(111)–P	121.6(7)
C(32)–Ru(3)–Ru(1)	96.2(3)	C(32)–Ru(3)–Ru(2)	145.9(2)	C(132)–C(131)–P	121.0(6)	C(136)–C(131)–P	118.4(6)
C(32)–Ru(3)–Cu	154.9(2)	C(32)–Ru(3)–C(1)	94.7(3)	C(122)–C(121)–P	119.0(6)	C(126)–C(121)–P	122.7(6)

all three ruthenium atoms *via* one σ bond to the 'wing-tip' ruthenium site and two π bonds to the two ruthenium atoms which form the 'body' of the 'butterfly'. Each ruthenium atom is ligated by three CO groups, which are all essentially terminal, except for CO(23) and CO(33) which exhibit short Cu–C contacts [2.552(7) and 2.496(7) Å, respectively]. However, the C–O bond lengths and the Ru–C–O angles of these latter CO groups are not significantly different from those of the others and there is no real evidence from i.r. spectroscopy to support any interaction between CO ligands and the coinage metals in (**10**) and (**11**) (Table 1). Similar close Cu–C contacts (2.30—2.73 Å) have been reported for some of the CO groups in the anion $[CuOs_{10}C(CO)_{24}(NCMe)]^-$ [6] and in $[Cu_2Ru_6C(CO)_{16}(NCMe)_2]$.[9] Short Au–C distances have also been observed [11,21,27] for CO ligands in some heteronuclear clusters containing bridging $Au(PR_3)$ fragments.

The C–C separations and Ru–C distances for the t-butylacetylide ligand in (**10**) are very similar to the corresponding vectors reported for the anion $[Ru_3(CO)_9(C_2Bu^t)]^-$ [28] and for a number of, structurally, very closely related compounds, in which the bridging $Cu(PPh_3)$ moiety is replaced by X [X = H,[26,29] $Au(PPh_3)$,[25] Hg,[30] $HgMo(CO)_3(\eta\text{-}C_5H_5)$,[30] HgBr,[31] or Cl[32]]. The Ru–Ru vector bridged by the $Cu(PPh_3)$ unit in (**10**) is *ca.* 0.1 Å longer than the equivalent separation in $[Ru_3(CO)_9(C_2Bu^t)]^-$,[28] compared to an increase in bond length of *ca.* 0.13 Å for a bridging hydrido ligand,[26] *ca.* 0.16 Å for a bridging $Au(PPh_3)$ moiety,[25] and *ca.* 0.61 Å for a bridging chlorine atom.[32] The two other Ru–Ru vectors in (**10**) are little different from the corresponding distances in $[Ru_3(CO)_9(C_2Bu^t)]^-$.[28]

While the work described herein was in progress, reports [11–13,16] appeared of a number of other heteronuclear clusters which were thought to contain a $Cu(PR_3)$ group bridging a metal–metal bond. However, to our knowledge, the only other such cluster which has been structurally characterized by a single-crystal *X*-ray diffraction study is the copper–osmium compound $[CuOs_3(\mu\text{-}H)_3(CO)_{10}(PPh_3)]$.[8]

Heteronuclear Group 1B *Metal Clusters synthesized from the Salt* $[N(PPh_3)_2][Fe_3(\mu\text{-}COMe)(CO)_{10}]$.—Treatment of a dichloromethane solution of the salt $[N(PPh_3)_2][Fe_3(\mu\text{-}COMe)(CO)_{10}]$ with $[MX(PPh_3)]$ (M = Cu or Au, X = Cl; M = Ag, X = I), in the presence of $TlPF_6$, affords another series of Group 1B metal congeners, the purple cluster compounds $[MFe_3(\mu\text{-}COMe)(CO)_{10}(PPh_3)]$ [M = Cu (**15**), Ag (**16**), or Au (**17**)]. The yields obtained for (**15**) and (**17**) are 44 and 65%, respectively, but the silver–iron cluster (**16**) could only be isolated as an oil and it decomposes very rapidly at room temperature, both as an oil and in solution. No satisfactory analytical, $^{31}P\text{-}\{^1H\}$, or $^{13}C\text{-}\{^1H\}$ n.m.r. data could be obtained

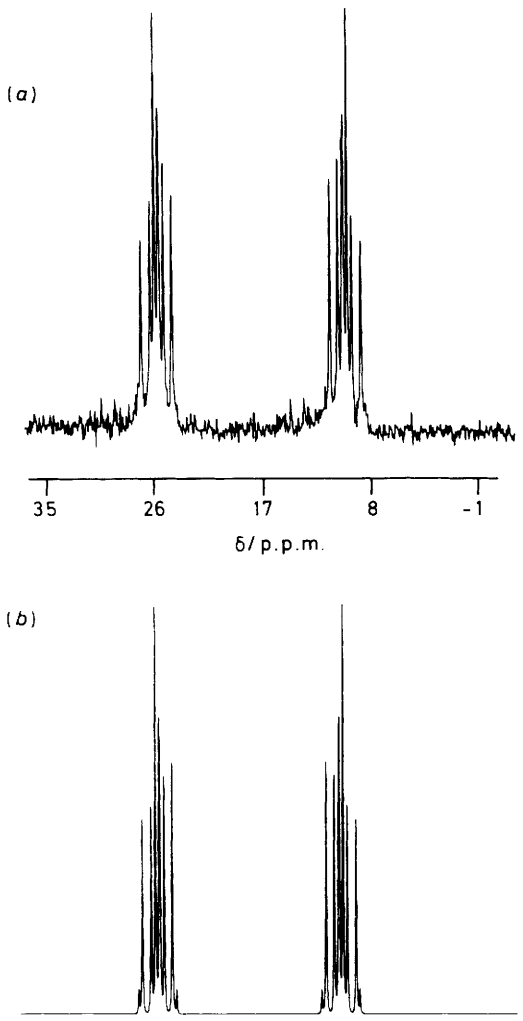

Figure 4. Observed (measured in $[^2H_2]$dichloromethane solution at −90 °C) (*a*) and simulated (*b*) $^{31}P-\{^1H\}$ n.m.r. spectra for $[\{AgRu_4(\mu_3\text{-}H)_3(CO)_{12}\}_2(\mu\text{-}Ph_2PCH_2CH_2PPh_2)]$ (**7**)

for (**16**), because of this temperature sensitivity. However, although the copper–iron cluster (**15**) is also rather unstable at ambient temperature, decomposing slowly in the solid state and quite rapidly in solution, it has been fully characterized (Tables 1, 2, and 3).

Hydrogen-1 and $^{13}C-\{^1H\}$ n.m.r. spectra for (**15**) and the ^1H n.m.r. spectra of (**16**) confirm that the bridging methoxymethylidyne ligand of the precursor is also present in these products. The $^{31}P-\{^1H\}$ n.m.r. spectrum of (**15**) shows a single phosphorus environment. The gold–iron cluster (**17**) has been previously prepared by a different route[27] and it is assumed to exhibit the same 'butterfly' metal-core structure as that adopted by its ruthenium analogue $[AuRu_3(\mu\text{-}COMe)(CO)_{10}(PPh_3)]$.[27] In the latter species, the gold atom occupies a 'wing-tip' site in the cluster and the methoxymethylidyne ligand bridges the Ru–Ru bond which forms the 'body' of the 'butterfly'. As the i.r. and n.m.r. spectroscopic data for (**15**) and (**16**) are closely similar to those reported[27] for (**17**), it would seem that the copper and silver iron clusters adopt the same geometry, with a $M(PPh_3)$ (M = Cu or Ag) fragment bridging a Fe–Fe bond.

N.M.R. Spectra of the Copper and Silver Heteronuclear Clusters. The ^1H and $^{31}P-\{^1H\}$ n.m.r. spectra of all the copper and silver mixed-metal clusters exhibit several additional interesting features which are worthy of further comment. At ambient temperature, quite severe broadening is visible for the $^{31}P-\{^1H\}$ n.m.r. singlet resonances of the copper–ruthenium species (**1**), (**2**), (**6**), and (**10**), but at −90 °C these peaks are much sharper (Table 2). Similar temperature-dependent broadening behaviour has been previously observed[5,33] for phosphorus atoms bonded directly to copper and it has been attributed to quadrupolar effects from the copper interfering with the higher temperature spectra.

The ^1H n.m.r. hydrido ligand signal of (**1**) is also rather broad at ambient temperature, although cooling to −30 °C changes it into a sharp doublet (Table 2). Quadrupolar broadening of the ^1H n.m.r. signals due to hydrido ligands bonded directly to copper has also been reported,[34] but it seems an unlikely explanation in this case, as the corresponding resonances for (**2**), (**6**), and $[CuMRu_4(\mu_3\text{-}H)_2(CO)_{12}(PPh_3)_2]$ (M = Cu or Ag)[5] show no such broadening at ambient temperature. The broadening for (**1**) probably arises from a fluxional process involving intermolecular exchange of $PMePh_2$ ligands between clusters, similar to that described below for the silver–ruthenium clusters.

For the silver–ruthenium clusters (**3**), (**7**), and (**11**), the $^{31}P-\{^1H\}$ n.m.r. spectra at −90 °C show additional splittings due to $^{107,109}Ag-^{31}P$ coupling. In the case of (**3**) and (**11**), which just contain one $Ag(PPh_3)$ unit, the $^{31}P-\{^1H\}$ n.m.r. resonance is only split into two doublets.[35] However, (**7**) contains an $AgPCH_2CH_2PAg$ fragment and the $^{31}P-\{^1H\}$ spectrum is more complicated [Figure 4(*a*)], because $^3J(PP)$ also contributes to the form of the spectrum as well as $^1J(^{107,109}AgP)$ and three different molecules of (**7**) are possible from the various combinations of the silver isotopes.[36] It is possible to simulate the three different sub-spectra, using the A part of an AA'XX' or AA'MX spin system,[36] as appropriate, and when these sub-spectra are summed, with the appropriate statistical weighting for the relative isotopic abundances, a good fit with the observed spectrum is obtained (Figure 4). For all these clusters, the observed ratios of $J(^{109}AgP)/J(^{107}AgP)$ and, where visible, $J(^{109}AgH)/J(^{107}AgH)$ are very close to the theoretical value of 1.149, which corresponds to the ratio of gyromagnetic ratios for the two silver isotopes.[35]

At ambient temperature, the $^{31}P-\{^1H\}$ resonances for (**3**), (**7**), and (**11**) are very severely broadened and, furthermore, no $^{31}P-^1H$ or $^{107,109}Ag-^1H$ coupling is visible on the ^1H n.m.r. hydrido ligand signals for (**3**) and (**7**). This broadening and loss of coupling suggests that, at ambient temperature in solution, the phosphine groups and, at least in the case of (**3**) and (**7**), also the silver atoms of these species are undergoing fluxional processes involving dissociative exchange between the clusters. Supporting the idea of the phosphine ligand exchange, when one equivalent of free PPh_3 is added to a sample of (**3**) in CD_2Cl_2, the $^{31}P-\{^1H\}$ n.m.r. spectrum of the mixture at −30 °C shows only one broad peak with a chemical shift intermediate between that of the $Ag(PPh_3)$ moiety in (**3**) and that of the free ligand. The detection of only one signal for an average PPh_3 environment demonstrates that PPh_3 groups bonded to the silver atoms in (**3**) can exchange with the free ligand in solution. Similar lability of phosphine groups bonded to silver atoms has been previously reported for a variety of different complexes[5,35,36] and an intermolecular fluxional process involving exchange of both silver atoms and phosphine ligands between some heteronuclear dimers is also known.[37]

Conclusions

A preference of $Cu(PR_3)$ moieties to cap triangular three-metal faces rather than to bridge metal–metal bonds is observed in one series of Group 1B metal congeners, as predicted from the molecular orbital calculations of Evans and Mingos.[3,4] However, stable heteronuclear clusters in which $M(PR_3)$ (M = Cu

or Ag) units bridge metal–metal bonds can also be readily prepared.

Experimental

All reactions and manipulations were performed under an atmosphere of dry oxygen-free nitrogen, using Schlenk-tube techniques.[38] Solvents were freshly distilled under nitrogen from the usual drying agents immediately before use. Light petroleum refers to that fraction of b.p. 40—60 °C. Established methods were used to prepare $[AuRu_3(CO)_9(C_2Bu^t)(PPh_3)]$,[25] $[N(PPh_3)_2][Ru_4(\mu\text{-}H)_3(CO)_{12}]$,[39] $[N(PPh_3)_2][Fe_3(\mu\text{-}COMe)(CO)_{10}]$,[40] $[Cu(NCMe)_4]PF_6$,[41] $[AgI(PPh_3)]$,[42] and $[Au_2(\mu\text{-}Ph_2PCH_2PPh_2)Cl_2]$.[43] The salt $[N(PPh_3)_2][Ru_3(CO)_9(C_2Bu^t)]$[28] and the complexes $[Ag(NCMe)_4]PF_6$,[41] $[CuCl(PPh_3)]$,[44] and $[AuCl(PPh_3)]$[45] were synthesized by adaptation of published routes. Analytical and other physical data for the new compounds are presented in Table 1, together with their i.r. spectra. Tables 2 and 3 summarize the results of n.m.r. spectroscopy measurements.

Infrared spectra were recorded on a Nicolet FT MX-1 spectrophotometer or a Perkin-Elmer 299B instrument. Hydrogen-1 and $^{13}C\text{-}\{^1H\}$ n.m.r. spectra were measured on JEOL FX 200, Bruker AM 250, or Bruker WH 400 spectrometers and $^{31}P\text{-}\{^1H\}$ n.m.r. spectra on JEOL FX 90Q, JEOL PS/PFT 100, or Bruker AM 250 instruments. Product separation by column chromatography was performed on Aldrich Florisil (100—200 mesh) or B.D.H. silica gel (60—120 mesh).

Synthesis of the Compounds $[MRu_4(\mu_3\text{-}H)_3(CO)_{12}L]$ (M = Cu, L = $PMePh_2$ *or* PPh_3; M = Ag, L = PPh_3) *and* $[\{MRu_4(\mu_3\text{-}H)_3(CO)_{12}\}_2(\mu\text{-}Ph_2PCH_2CH_2PPh_2)]$ (M = Cu *or* Ag).—A dichloromethane (50 cm^3) solution of $[N(PPh_3)_2][Ru_4(\mu\text{-}H)_3(CO)_{12}]$ (1.00 g, 0.78 mmol) at −30 °C was treated with a solution of $[Cu(NCMe)_4]PF_6$ (0.29 g, 0.79 mmol) in dichloromethane (30 cm^3) and then, after stirring the reaction mixture at −30 °C for 1 min, a dichloromethane (20 cm^3) solution of $PMePh_2$ (0.16 g, 0.80 mmol) was added. The mixture was allowed to warm to ambient temperature with stirring and the solvent removed under reduced pressure. The crude residue was extracted with diethyl ether–light petroleum (1:1; 50-cm^3 portions) until the extracts were no longer orange and the combined extracts were then filtered through a Celite pad (*ca.* 1 × 3 cm). After removal of the solvent under reduced pressure, the residue was dissolved in dichloromethane–light petroleum (1:3) and chromatographed at −20 °C on a Florisil column (20 × 3 cm). Elution with dichloromethane–light petroleum (1:3) afforded one dark orange fraction, which, after removal of the solvent under reduced pressure and crystallization of the residue from dichloromethane–light petroleum, yielded dark orange *microcrystals* of $[CuRu_4(\mu_3\text{-}H)_3(CO)_{12}(PMePh_2)]$ (**1**) (0.62 g).

Dark orange *microcrystals* of $[CuRu_4(\mu_3\text{-}H)_3(CO)_{12}(PPh_3)]$ (**2**) (0.64 g) and $[\{CuRu_4(\mu_3\text{-}H)_3(CO)_{12}\}_2(\mu\text{-}Ph_2PCH_2CH_2PPh_2)]$ (**6**) (0.56 g) were synthesized by the same procedure using PPh_3 (0.21 g, 0.80 mmol) or $Ph_2PCH_2CH_2PPh_2$ (0.16 g, 0.40 mmol), respectively. The crude sample of (**6**) was dissolved in a 2:3 rather than a 1:3 dichloromethane–light petroleum mixture immediately before chromatography and the same solvent mixture was used for elution. The silver–ruthenium clusters $[AgRu_4(\mu_3\text{-}H)_3(CO)_{12}(PPh_3)]$ (**3**) (0.60 g) and $[\{AgRu_4(\mu_3\text{-}H)_3(CO)_{12}\}_2(\mu\text{-}Ph_2PCH_2CH_2PPh_2)]$ (**7**) (0.57 g) were similarly obtained, as dark orange *microcrystals*, using $[Ag(NCMe)_4]PF_6$ (0.33 g, 0.79 mmol) in place of $[Cu(NCMe)_4]PF_6$, and PPh_3 (0.21 g, 0.80 mmol) or $Ph_2PCH_2CH_2PPh_2$ (0.16 g, 0.40 mmol), respectively. The chromatography conditions for (**7**) were the same as those for (**6**).

Alternatively, compounds (**2**) (0.39 g, 67%) and (**3**) (0.38 g, 62%) can also be synthesized, in slightly reduced yield, by the route described below for the gold-ruthenium cluster (**8**). The complexes $[CuCl(PPh_3)]$ (0.20 g, 0.55 mmol) or $[AgI(PPh_3)]$ (0.27 g, 0.55 mmol), were utilized for (**2**) and (**3**), respectively, instead of $[AuCl(PPh_3)]$, and the conditions employed for chromatography and crystallization were the same as those described above.

Synthesis of the Compounds $[AuRu_4(\mu\text{-}H)_3(CO)_{12}(PPh_3)]$ *and* $[\{AuRu_4(\mu\text{-}H)_3(CO)_{12}\}_2(\mu\text{-}Ph_2PCH_2PPh_2)]$.—A dichloromethane (50 cm^3) solution of $[N(PPh_3)_2][Ru_4(\mu\text{-}H)_3(CO)_{12}]$ (0.70 g, 0.55 mmol) was treated with $[AuCl(PPh_3)]$ (0.27 g, 0.55 mmol) and $TlPF_6$ (0.60 g, 1.72 mmol) and the mixture stirred at room temperature for 0.25 h. After filtration of the red mixture through a Celite pad (*ca.* 1 × 3 cm), the solvent was removed under reduced pressure and the crude residue dissolved in dichloromethane–light petroleum (1:4). Chromatography on a Florisil column (15 × 3 cm), eluting with dichloromethane–light petroleum (1:4), afforded an orange fraction containing the product. After removal of the solvent under reduced pressure, crystallization of the residue from dichloromethane–light petroleum yielded dark orange *microcrystals* of $[AuRu_4(\mu\text{-}H)_3(CO)_{12}(PPh_3)]$ (**8**) (0.46 g).

Dark orange *microcrystals* of $[\{AuRu_4(\mu\text{-}H)_3(CO)_{12}\}_2(\mu\text{-}Ph_2PCH_2PPh_2)]$ (**9**) (0.36 g) were similarly prepared, using $[Au_2(\mu\text{-}Ph_2PCH_2PPh_2)Cl_2]$ (0.47 g, 0.55 mmol). The crude product was dissolved in a 2:3 rather than a 1:4 dichloromethane–light petroleum mixture and chromatographed on a Florisil column (20 × 3 cm) at −20 °C. Elution with dichloromethane–light petroleum (2:3) afforded a dark orange fraction containing the product, followed by a red fraction containing $[Au_2Ru_4(\mu_3\text{-}H)(\mu\text{-}H)(\mu\text{-}Ph_2PCH_2PPh_2)(CO)_{12}]$ (0.08 g, 10%). Both fractions were worked-up as above.

Synthesis of the Compounds $[MRu_3(CO)_9(C_2Bu^t)(PPh_3)]$ (M = Cu *or* Ag).—Following the procedure described for (**1**), a dichloromethane (40 cm^3) solution of $[N(PPh_3)_2][Ru_3(CO)_9(C_2Bu^t)]$ (0.56 g, 0.48 mmol) was first treated with $[Cu(NCMe)_4]PF_6$ (0.18 g, 0.48 mmol) in dichloromethane (20 cm^3) and then with a dichloromethane (20 cm^3) solution of PPh_3 (0.13 g, 0.50 mmol). Again as for (**1**), the product was extracted until the extracts were no longer yellow and the combined extracts were filtered. After removal of the solvent under reduced pressure, the crude residue was dissolved in dichloromethane–light petroleum (1:4) and chromatographed at −20 °C on a Florisil column (20 × 3 cm), eluting with dichloromethane–light petroleum (1:4). One yellow fraction was collected, which, after removal of the solvent under reduced pressure and crystallization of the residue from light petroleum, yielded yellow *crystals* of $[CuRu_3(CO)_9(C_2Bu^t)(PPh_3)]$ (**10**) (0.34 g).

Yellow *crystals* of $[AgRu_3(CO)_9(C_2Bu^t)(PPh_3)]$ (**11**) (0.32 g) were prepared using the above procedure with $[Ag(NCMe)_4]PF_6$ (0.20 g 0.48 mmol). Alternatively, reduced yields of (**10**) (0.13 g, 40%) and (**11**) (0.12 g, 35%) can be obtained by treating a dichloromethane (40 cm^3) solution of $[N(PPh_3)_2][Ru_3(CO)_9(C_2Bu^t)]$ (0.40 g, 0.34 mmol) with $[CuCl(PPh_3)]$ (0.13 g, 0.36 mmol) or $[AgI(PPh_3)]$ (0.18 g, 0.36 mmol), respectively, in the presence of $TlPF_6$ (0.24 g, 0.69 mmol). The procedure previously described for (**8**) was used to afford the crude products, which were then purified as above.

Synthesis of the Compounds $[MFe_3(\mu\text{-}COMe)(CO)_{10}(PPh_3)]$ (M = Cu *or* Ag).—A dichloromethane (30 cm^3) solution of $[N(PPh_3)_2][Fe_3(\mu\text{-}COMe)(CO)_{10}]$ (0.40 g, 0.39 mmol) at 0 °C was treated with $[CuCl(PPh_3)]$ (0.28 g, 0.78 mmol) and $TlPF_6$ (0.60 g, 1.72 mmol) and the mixture stirred at 0 °C for 0.5 h. After removal of the solvent under reduced pressure at the

Table 6. Atomic positional parameters (fractional co-ordinates) for $[CuRu_4(\mu_3\text{-}H)_3(CO)_{12}(PMePh_2)]$ (**1**), with estimated standard deviations in parentheses

Atom	*x*	*y*	*z*	Atom	*x*	*y*	*z*
Ru(1)	0.178 61(6)	0.231 93(2)	0.154 27(3)	O(33)	0.282 0(8)	0.186 9(2)	−0.100 4(3)
Ru(2)	−0.144 14(6)	0.184 04(2)	0.160 42(3)	C(41)	0.062 3(9)	0.289 7(3)	−0.051 3(4)
Ru(3)	0.065 11(6)	0.144 40(2)	0.030 02(3)	O(41)	0.128 5(7)	0.310 2(2)	−0.103 1(3)
Ru(4)	−0.057 87(6)	0.256 85(2)	0.032 07(3)	C(42)	−0.237 0(9)	0.247 2(3)	−0.042 5(4)
Cu	0.123 31(10)	0.119 94(3)	0.196 51(5)	O(42)	−0.342 6(7)	0.242 9(3)	−0.088 1(4)
P	0.196 66(19)	0.042 21(7)	0.267 72(10)	C(43)	−0.128 8(8)	0.329 5(3)	0.066 5(4)
C(11)	0.337 9(8)	0.209 7(3)	0.240 4(4)	O(43)	−0.175 9(7)	0.374 2(2)	0.084 3(4)
O(11)	0.438 9(6)	0.199 7(3)	0.286 8(3)	H(512)	0.036 6(71)	0.194 0(25)	0.221 9(36)
C(12)	0.323 9(9)	0.266 8(3)	0.083 4(4)	H(513)	0.215 0(70)	0.163 1(25)	0.105 6(36)
O(12)	0.414 5(7)	0.286 3(3)	0.044 1(4)	H(523)	−0.051 6(73)	0.123 0(24)	0.115 8(37)
C(13)	0.125 3(8)	0.305 2(3)	0.199 0(5)	C(1)	0.040 0(9)	−0.012 6(3)	0.263 5(5)
O(13)	0.095 5(7)	0.348 3(2)	0.227 9(4)	C(111)	0.249 5(8)	0.051 9(3)	0.377 4(4)
C(21)	−0.191 2(8)	0.137 2(3)	0.256 5(4)	C(112)	0.401 9(10)	0.064 3(3)	0.404 8(5)
O(21)	−0.227 4(7)	0.113 0(3)	0.313 0(4)	C(113)	0.443 8(14)	0.073 0(4)	0.490 3(7)
C(22)	−0.329 2(8)	0.166 5(3)	0.095 0(5)	C(114)	0.331 9(12)	0.069 4(4)	0.544 8(6)
O(22)	−0.440 3(6)	0.153 8(3)	0.057 4(4)	C(115)	0.181 8(13)	0.059 0(4)	0.521 2(6)
C(23)	−0.231 0(9)	0.254 1(3)	0.199 7(5)	C(116)	0.134 7(11)	0.049 1(4)	0.436 1(5)
O(23)	−0.289 4(8)	0.294 4(2)	0.224 8(5)	C(121)	0.366 0(7)	0.005 3(3)	0.228 1(4)
C(31)	0.141 4(8)	0.065 2(3)	0.031 8(4)	C(122)	0.463 3(9)	0.035 1(3)	0.178 9(5)
O(31)	0.179 0(8)	0.018 5(2)	0.023 8(4)	C(123)	0.595 0(11)	0.008 2(4)	0.148 0(5)
C(32)	−0.099 0(10)	0.130 1(3)	−0.051 8(5)	C(124)	0.627 1(11)	−0.048 8(4)	0.167 7(5)
O(32)	−0.193 2(9)	0.118 7(3)	−0.100 8(4)	C(125)	0.529 3(9)	−0.079 5(3)	0.217 3(5)
C(33)	0.197 7(10)	0.171 7(3)	−0.052 1(4)	C(126)	0.399 4(8)	−0.052 8(3)	0.248 2(4)

Table 7. Atomic positional parameters (fractional co-ordinates) for $[CuRu_3(CO)_9(C_2Bu^t)(PPh_3)]$ (**10**), with estimated standard deviations in parentheses

Atom	*x*	*y*	*z*	Atom	*x*	*y*	*z*
Ru(1)	0.254 62(4)	0.125 08(3)	−0.094 01(4)	C(32)	0.287 7(5)	0.312 0(5)	0.029 9(6)
Ru(2)	0.208 61(4)	0.208 38(3)	−0.273 11(4)	O(32)	0.288 1(5)	0.325 4(4)	0.105 5(4)
Ru(3)	0.291 39(4)	0.287 96(3)	−0.099 09(4)	C(33)	0.415 8(5)	0.259 2(5)	−0.049 2(5)
Cu	0.369 50(6)	0.271 05(6)	−0.231 47(7)	O(33)	0.490 9(4)	0.241 9(4)	−0.013 8(4)
C(1)	0.168 9(4)	0.212 0(4)	−0.140 5(5)	P	0.491 24(13)	0.283 88(12)	−0.276 87(15)
C(2)	0.141 3(4)	0.280 2(4)	−0.184 3(5)	C(111)	0.549 0(5)	0.188 8(4)	−0.272 1(6)
C(3)	0.061 3(5)	0.335 8(5)	−0.207 4(6)	C(112)	0.578 6(6)	0.148 9(5)	−0.185 3(6)
C(301)	−0.024 7(6)	0.286 4(6)	−0.257 3(8)	C(113)	0.623 3(6)	0.076 9(6)	−0.177 1(7)
C(302)	0.064 7(7)	0.404 0(6)	−0.277 0(8)	C(114)	0.639 3(6)	0.045 9(6)	−0.255 4(7)
C(303)	0.059 6(8)	0.369 5(8)	−0.110 0(7)	C(115)	0.606 0(7)	0.08 33(7)	−0.343 5(8)
C(11)	0.187 4(6)	0.031 5(5)	−0.135 4(6)	C(116)	0.559 8(7)	0.155 8(6)	−0.354 0(7)
O(11)	0.142 0(5)	−0.024 1(4)	−0.158 4(6)	C(121)	0.466 9(5)	0.320 5(4)	−0.400 2(5)
C(12)	0.263 5(5)	0.116 0(5)	0.039 7(7)	C(122)	0.385 0(6)	0.301 4(6)	−0.470 2(7)
O(12)	0.264 5(5)	0.114 2(4)	0.117 4(5)	C(123)	0.360 9(7)	0.330 6(6)	−0.566 7(8)
C(13)	0.370 7(6)	0.077 8(5)	−0.081 3(6)	C(124)	0.419 4(7)	0.377 9(6)	−0.591 7(8)
O(13)	0.440 5(5)	0.054 4(4)	−0.075 0(5)	C(125)	0.501 8(8)	0.398 2(7)	−0.525 8(8)
C(21)	0.192 4(5)	0.289 7(5)	−0.371 2(5)	C(126)	0.526 8(7)	0.369 6(6)	−0.427 4(7)
O(21)	0.184 0(4)	0.335 6(4)	−0.430 3(5)	C(131)	0.580 1(5)	0.348 4(4)	−0.199 1(5)
C(22)	0.106 8(5)	0.143 8(4)	−0.344 5(6)	C(132)	0.670 5(6)	0.334 0(6)	−0.185 5(7)
O(22)	0.047 1(4)	0.103 6(3)	−0.385 4(5)	C(133)	0.735 7(7)	0.386 1(6)	−0.122 5(7)
C(23)	0.292 6(5)	0.141 0(5)	−0.304 6(6)	C(134)	0.710 6(7)	0.446 8(6)	−0.077 2(8)
O(23)	0.338 1(4)	0.097 1(3)	−0.328 5(5)	C(135)	0.621 1(7)	0.461 7(6)	−0.091 3(8)
C(31)	0.301 7(5)	0.395 4(5)	−0.136 3(6)	C(136)	0.554 9(6)	0.411 4(5)	−0.153 3(7)
O(31)	0.310 2(5)	0.460 3(3)	−0.154 2(5)				

same temperature, the crude residue was extracted with light petroleum (4 × 40 cm^3) at 0 °C and filtered through a Celite pad (*ca.* 1 × 3 cm). Reduction of the volume of the resultant purple solution to *ca.* 5 cm^3 under reduced pressure at 0 °C and subsequent cooling to −20 °C yielded purple *microcrystals* of $[CuFe_3(\mu\text{-}COMe)(CO)_{10}(PPh_3)]$ (**15**) (0.14 g). The product decomposed at room temperature, slowly in the solid state, and quite rapidly in solution.

Performing the above procedure at −40 °C, using the complex [AgI(PPh_3)] (0.39 g, 0.78 mmol) instead of $[CuCl(PPh_3)]$ yielded $[AgFe_3(\mu\text{-}COMe)(CO)_{10}(PPh_3)]$ (**16**), but crystallization of the product did not prove possible. However, (**16**) was obtained as a purple oil by removing the solvent under reduced pressure from the filtered purple extracts at −40 °C. The compound decomposed very rapidly at room temperature, both as an oil and in solution.

Synthesis of the Compound $[AuFe_3(\mu\text{-}COMe)(CO)_{10}(PPh_3)]$.—A dichloromethane (40 cm^3) solution of $[N(PPh_3)_2][Fe_3(\mu\text{-}COMe)(CO)_{10}]$ (0.40 g, 0.39 mmol) was treated with $[AuCl(PPh_3)]$ (0.39 g, 0.78 mmol) and $TlPF_6$ (0.60 g, 1.72 mmol), using the procedure previously described for (**8**) until the chromatography, which was performed on a silica gel column (15 × 3 cm), eluting with dichloromethane–light petroleum (1:4). One purple fraction was collected, which, after removal of the solvent under reduced pressure and crystallization of the residue from light petroleum, yielded purple *microcrystals* of $[AuFe_3(\mu\text{-}COMe)(CO)_{10}(PPh_3)]$ (**17**) (0.24 g, 65%).

Crystal Structure Determinations.—Crystals of $[CuRu_4(\mu_3\text{-}H)_3(CO)_{12}(PMePh_2)]$ (**1**) and $[CuRu_3(CO)_9(C_2Bu^t)(PPh_3)]$ (**10**) were grown from light petroleum solutions by slow evaporation and subsequent cooling to −20 °C.

The crystals selected for data collection had dimensions 0.28 × 0.18 × 0.12 mm for (**1**) and 0.23 × 0.16 × 0.14 mm for (**10**). The methods of data collection, data processing, and absorption correction used were similar to those described previously.[46] A scan width of 0.8° was used to collect data in the θ range 3—25° for both crystals. Equivalent reflections were averaged to give 4 161 and 4 070 unique absorption corrected data, with $I/\sigma(I) > 3.0$, for (**1**) and (**10**), respectively.

Crystal data. For (**1**). $[CuRu_4(\mu_3\text{-}H)_3(CO)_{12}(PMePh_2)]$, $C_{25}H_{16}CuO_{12}PRu_4$, M = 1 007.19, monoclinic, space group $P2_1/c$, a = 8.517(3), b = 23.050(4), c = 16.050(4) Å, β = 93.29(4)°, U = 3 145.69 Å^3, Z = 4, $F(000)$ = 1 928, μ(Mo-K_α) = 24.46 cm^{-1}, D_c = 2.126 g cm^{-3}, Mo-K_α radiation, λ = 0.710 69 Å.

For (**10**). $[CuRu_3(CO)_9(C_2Bu^t)(PPh_3)]$, $C_{33}H_{24}CuO_9PRu_3$, M = 962.28, monoclinic, space group $P2_1/n$, a = 15.605(4), b = 16.839(4), c = 14.449(3) Å, β = 109.42(4)°, U = 3 580.79 Å^3, Z = 4, $F(000)$ = 1 880, μ(Mo-K_α) = 17.73 cm^{-1}, D_c = 1.784 g cm^{-3}, Mo-K_α radiation, λ = 0.710 69 Å.

Structure solution and refinement.[47] For both (**1**) and (**10**), the positions of the metal atoms were determined from Patterson syntheses. The remaining non-hydrogen atoms were found from subsequent difference Fourier maps. For (**1**) and (**10**), the Cu, Ru, P, O, and carbonyl carbon atoms were assigned anisotropic thermal parameters, together with the C_2Bu^t carbon atoms in the structure of (**10**). For (**1**), the hydride hydrogen atoms were located from difference maps and were successfully refined isotropically. For both structures, the remaining C–H hydrogen atoms were included in the structure factor calculations at calculated positions with C–H = 1.08 Å.

Final R and R' values of 0.0324 and 0.0343 were obtained for (**1**) and of 0.0388 and 0.0399 for (**10**), respectively. The final atomic positional parameters for compounds (**1**) and (**10**) (excluding those of the phosphine ligand hydrogen atoms) are listed in Tables 6 and 7, respectively.

Acknowledgements

One of us (I. D. S.) gratefully acknowledges the support and guidance given to him by Professor F. G. A. Stone, F. R. S., during some of the experiments described herein. In addition, we thank Dr. M. Murray for the simulation of the $^{31}P\text{-}\{^1H\}$ n.m.r. spectrum, Drs. O. W. Howarth and E. H. Curzon for recording a number of 400-MHz ^1H n.m.r. spectra, Dr. B. F. G. Johnson and Mr. R. M. Sorrell for communication of unpublished spectroscopic data, the Nuffield Foundation for partial support of the work, Johnson Matthey Ltd. for a generous loan of gold, silver, and ruthenium salts, Mr. R. J. Lovell for technical assistance, and Mrs. L. J. Salter for drawing the diagrams.

References

1 For example, K. P. Hall and D. M. P. Mingos, *Prog. Inorg. Chem.*, 1984, **32**, 237; P. Braunstein and J. Rose, *Gold Bull.*, 1985, **18**, 17 and refs. therein.
2 J. A. K. Howard, I. D. Salter, and F. G. A. Stone, *Polyhedron*, 1984, **3**, 567 and refs. therein.
3 D. G. Evans and D. M. P. Mingos, *J. Organomet. Chem.*, 1982, **232**, 171.
4 D. M. P. Mingos, *Polyhedron*, 1984, **3**, 1289.
5 M. J. Freeman, M. Green, A. G. Orpen, I. D. Salter, and F. G. A. Stone, *J. Chem. Soc., Chem. Commun.*, 1983, 1332.
6 B. F. G. Johnson, J. Lewis, W. J. H. Nelson, M. D. Vargas, D. Braga, and M. McPartlin, *J. Organomet. Chem.*, 1983, **246**, C69.
7 D. Braga, K. Henrick, B. F. G. Johnson, J. Lewis, M. McPartlin, W. J. H. Nelson, A. Sironi, and M. D. Vargas, *J. Chem. Soc., Chem. Commun.*, 1983, 1131.
8 B. F. G. Johnson, J. Lewis, P. R. Raithby, S. N. A. B. Syed-Mustaffa, M. J. Taylor, K. H. Whitmire, and W. Clegg, *J. Chem. Soc., Dalton Trans.*, 1984, 2111.
9 J. S. Bradley, R. L. Pruett, E. Hill, G. B. Ansell, M. E. Leonowicz, and M. A. Modrick, *Organometallics*, 1982, **1**, 748.
10 G. B. Ansell, M. A. Modrick, and J. S. Bradley, *Acta Crystallogr., Sect. C*, 1984, **40**, 365.
11 J. A. Iggo, M. J. Mays, P. R. Raithby, and K. Henrick, *J. Chem. Soc., Dalton Trans.*, 1984, 633.
12 M. J. Mays, P. R. Raithby, P. L. Taylor, and K. Henrick, *J. Chem. Soc., Dalton Trans.*, 1984, 959.
13 P. Braunstein, J. Rose, A. M. Manotti-Lanfredi, A. Tiripicchio, and E. Sappa, *J. Chem. Soc., Dalton Trans.*, 1984, 1843.
14 P. Braunstein and J. Rose, *J. Organomet. Chem.*, 1984, **262**, 223.
15 C. P. Horwitz, E. M. Holt, and D. F. Shriver, *J. Am. Chem. Soc.*, 1985, **107**, 281.
16 M. I. Bruce, E. Horn, J. G. Matisons, and M. R. Snow, *J. Organomet. Chem.*, 1985, **286**, 271.
17 I. D. Salter and F. G. A. Stone, *J. Organomet. Chem.*, 1984, **260**, C71.
18 S. S. D. Brown, I. D. Salter, and B. M. Smith, *J. Chem. Soc., Chem. Commun.*, 1985, 1439.
19 S. A. Bezman, M. R. Churchill, J. A. Osborn, and J. Wormald, *J. Am. Chem. Soc.*, 1971, **93**, 2063.
20 I. D. Salter, Ph.D. Thesis, University of Bristol, 1983.
21 B. F. G. Johnson, D. A. Kaner, J. Lewis, P. R. Raithby, and M. J. Taylor, *J. Chem. Soc., Chem. Commun.*, 1982, 314.
22 B. F. G. Johnson, D. A. Kaner, and J. Lewis, unpublished work.
23 R. D. Wilson, S. M. Wu, R. A. Love, and R. Bau, *Inorg. Chem.*, 1978, **17**, 1271.
24 M. I. Bruce and B. K. Nicholson, *J. Organomet. Chem.*, 1983, **252**, 243.
25 P. Braunstein, G. Predieri, A. Tiripicchio, and E. Sappa, *Inorg. Chim. Acta*, 1982, **63**, 113.
26 M. Catti, G. Gervasio, and S. A. Mason, *J. Chem. Soc., Dalton Trans.*, 1977, 2260.
27 L. W. Bateman, M. Green, K. A. Mead, R. M. Mills, I. D. Salter, F. G. A. Stone, and P. Woodward, *J. Chem. Soc., Dalton Trans.*, 1983, 2599.
28 C. Barner-Thorsen, K. I. Hardcastle, E. Rosenberg, J. Siegel, A. M. Manotti Lanfredi, A. Tiripicchio, and M. Tiripicchio Camellini, *Inorg. Chem.*, 1981, **20**, 4306.
29 A. J. Carty, S. A. MacLaughlin, N. J. Taylor, and E. Sappa, *Inorg. Chem.*, 1981, **20**, 4437.
30 S. Ermer, K. King, K. I. Hardcastle, E. Rosenberg, A. M. Manotti-Lanfredi, A. Tiripicchio, and M. Tiripicchio Camellini, *Inorg. Chem.*, 1983, **22**, 1339.
31 R. Fahmy, K. King, E. Rosenberg, A. Tiripicchio, and M. Tiripicchio Camellini, *J. Am. Chem. Soc.*, 1980, **102**, 3626.
32 S. Aime, D. Osella, A. J. Deeming, A. M. Manotti-Lanfredi, and A. Tiripicchio, *J. Organomet. Chem.*, 1983, **244**, C47.
33 G. V. Goeden and K. G. Caulton, *J. Am. Chem. Soc.*, 1981, **103**, 7354.
34 L. F. Rhodes, J. C. Huffman, and K. G. Caulton, *J. Am. Chem. Soc.*, 1985, **107**, 1759.
35 E. L. Muetterties and C. W. Alegranti, *J. Am. Chem. Soc.*, 1972, **94**, 6386.
36 A. F. M. J. van der Ploeg and G. van Koten, *Inorg. Chim. Acta*, 1981, **51**, 225.
37 M. Green, A. G. Orpen, I. D. Salter, and F. G. A. Stone, *J. Chem. Soc., Dalton Trans.*, 1984, 2497.
38 D. F. Shriver, 'The Manipulation of Air-Sensitive Compounds,' McGraw-Hill, New York, 1969.
39 K. E. Inkrott and S. G. Shore, *Inorg. Chem.*, 1979, **18**, 2817.
40 H. A. Hodali and D. F. Shriver, *Inorg. Chem.*, 1979, **18**, 1236.
41 G. J. Kubas, *Inorg. Synth.*, 1979, **19**, 90.
42 B-K. Teo and J. C. Calabrese, *Inorg. Chem.*, 1976, **15**, 2474.
43 H. Schmidbauer, W. Wohlleben, F. Wagner, O. Orama, and G. Huttner, *Chem. Ber.*, 1977, **110**, 1748.
44 G. B. Kauffman and L. A. Teter, *Inorg. Synth.*, 1963, **7**, 9.
45 F. G. Mann, A. F. Wells, and D. Purdie, *J. Chem. Soc.*, 1937, 1828.
46 K. Henrick, M. McPartlin, A. J. Deeming, S. Hasso, and P. Manning, *J. Chem. Soc., Dalton Trans.*, 1982, 889.
47 G. M. Sheldrick, SHELX76, Crystal Structure Solving Package, University of Cambridge, 1976.

Received 11*th October* 1985; *Paper* 5/1764